The Plant Cell, Vol. 32: 2402–2423, July 2020, www.plantcell.org © 2020 ASPB.

Molecular Basis for a Cell Fate Switch in Response to Impaired Ribosome Biogenesis in the Arabidopsis Root Epidermis

Wenjia Wang,[a,b,c] Kook Hui Ryu,[a] Angela Bruex,[a] Christa Barron,[a] and John Schiefelbein[a,1]

[a] Department of Molecular, Cellular, and Developmental Biology, University of Michigan, Ann Arbor, Michigan 48109
[b] Joint BioEnergy Institute, Emeryville, California 94608
[c] Environmental Genomics and Systems Biology Division, Lawrence Berkeley National Laboratory, Berkeley, California 94720

ORCID IDs: 0000-0002-4809-251X (W.W.); 0000-0002-0400-4493 (K.H.R.); 0000-0002-5342-4048 (A.B.); 0000-0002-9479-0503 (C.B.); 0000-0002-0560-5872 (J.S.)

The Arabidopsis (*Arabidopsis thaliana*) root epidermis consists of a position-dependent pattern of root hair cells and non-hair cells. Underlying this cell type patterning is a network of transcription factors including a central MYB-basic helix-loop-helix-WD40 complex containing WEREWOLF (WER), GLABRA3 (GL3)/ENHANCER OF GLABRA3, and TRANSPARENT TESTA GLABRA1. In this study, we used a genetic enhancer screen to identify *apum23-4*, a mutant allele of the ribosome biogenesis factor (RBF) gene *ARABIDOPSIS PUMILIO23* (*APUM23*), which caused prospective root hair cells to instead adopt the non-hair cell fate. We discovered that this cell fate switch relied on MYB23, a MYB protein encoded by a WER target gene and acting redundantly with WER. In the *apum23-4* mutant, *MYB23* exhibited ectopic expression that was WER independent and instead required ANAC082, a recently identified ribosomal stress response mediator. We examined additional RBF mutants that produced ectopic non-hair cells and determined that this cell fate switch is generally linked to defects in ribosome biogenesis. Furthermore, the flagellin peptide flg22 triggers the ANAC082-MYB23-GL2 pathway. Taken together, our study provides a molecular explanation for root epidermal cell fate switch in response to ribosomal defects and, more generally, it demonstrates a novel regulatory connection between stress conditions and cell fate control in plants.

INTRODUCTION

The development of multicellular organisms relies on the appropriate specification of distinct cell types. In the Arabidopsis (*Arabidopsis thaliana*) root epidermis, the root hair and non-hair cell types are specified in a position-dependent manner (Duckett et al., 1994; Clowes, 2000): epidermal cells adjacent to two underlying cortical cells (in the H position) adopt the root hair cell fate, while those adjacent to only one underlying cortical cell (in the N position) adopt the non-hair cell fate. This simple patterning system has been used as a model to uncover molecular mechanisms responsible for cell fate specification in plants (Masucci et al., 1996; Lee and Schiefelbein, 1999).

Previous genetic and molecular studies have revealed a network of transcription factors underlying root epidermal cell patterning. In N-position cells, WEREWOLF (WER), GLABRA3/ENHANCER OF GLABRA3 (GL3/EGL3), and TRANSPARENT TESTA GLABRA1 (TTG1) form a MYB-basic helix-loop-helix (bHLH)-WD40 complex (Galway et al., 1994; Lee and Schiefelbein, 1999; Bernhardt et al., 2003, 2005). This complex directly promotes transcription of *GL2*, encoding a homeodomain-leucine zipper transcription factor, and *CAPRICE* (*CPC*), encoding an R3-type MYB protein (Ryu et al., 2005; Song et al., 2011). The GL2 protein accumulates in the N-position cells and directly suppresses expression of downstream root hair–promoting genes (Masucci et al., 1996; Bruex et al., 2012; Lin et al., 2015). The CPC protein is able to translocate to the adjacent H-position cells and bind to GL3/EGL3 in competition with WER (Wada et al., 2002; Kurata et al., 2005; Song et al., 2011). In addition, a receptor-like kinase, SCRAMBLED (SCM), preferentially accumulates in H-position cells and further reduces WER-GL3/EGL3-TTG1 complex formation through suppressing *WER* expression (Kwak et al., 2005; Kwak and Schiefelbein, 2008). As a consequence, *GL2* expression is relatively weak in H-position cells, allowing for transcription of root hair–promoting genes and resulting in root hair cell differentiation (Cvrčková et al., 2010; Bruex et al., 2012; Huang et al., 2017).

The preferential accumulation of the WER-GL3/EGL3-TTG1 complex in N-position cells is reinforced by multiple feedback mechanisms (Schiefelbein et al., 2014). One of these feedback mechanisms involves MYB23, a close relative of WER (Stracke et al., 2001; Kang et al., 2009). The WER-GL3/EGL3-TTG1 complex directly promotes *MYB23* transcription in N-position cells, and the MYB23 protein is functionally redundant with WER (Kang et al., 2009). Thus, MYB23 acts in a positive feedback loop to ensure sufficient levels of the WER/MYB23 proteins for the MYB-bHLH-WD40 complex in N-position cells.

The proper differentiation of the root hair and non-hair cells, like essentially all developmental processes, relies on the production and function of ribosomes. Ribosome biogenesis, including precursor rRNA (pre-rRNA) processing and ribosomal protein (RP) assembly, involves the organized cooperation of numerous ribosome biogenesis factors (RBFs) (Thomson et al., 2013; Weis et al., 2015a; Sáez-Vásquez and Delseny, 2019). In Arabidopsis, mutants of RBF genes have significant developmental impacts,

[1] Address correspondence to schiefel@umich.edu.
The author responsible for the distribution of materials integral to the findings presented in this article in accordance with the policy described in the Instructions for Authors (www.plantcell.org) is: John Schiefelbein (schiefel@umich.edu).
www.plantcell.org/cgi/doi/10.1105/tpc.19.00773

including embryo lethality, aborted gametophyte development, and tissue regeneration defects (Harscoët et al., 2010; Ohbayashi et al., 2011; Missbach et al., 2013), as well as milder phenotypes such as retarded plant growth, merged or triple cotyledons, and narrow and pointed rosette leaves (Lange et al., 2011; Weis et al., 2014, 2015b). Interestingly, several characteristic phenotypes, such as the misshaped rosette leaves, are shared by mutants of functionally unrelated RBFs (Weis et al., 2015a), suggesting a common regulatory mechanism that responds to a variety of ribosome biogenesis defects and modulates plant development.

Recently, the *anac082-1* mutant, a missense mutation of the NAC family gene *ANAC082*, was reported to rescue the regeneration defects and the pointed-leaf phenotypes of several RBF mutants (Ohbayashi et al., 2017). Interestingly, the rescued double mutants still exhibit impaired pre-rRNA processing similar to the corresponding RBF single mutants (Ohbayashi et al., 2017), which implies that these developmental phenotypes are not directly caused by defective ribosome biogenesis. Therefore, ANAC082 is considered to be a key component of a regulatory response pathway in plants that connects ribosomal status with specific developmental events (Ohbayashi et al., 2017; Salomé, 2017; Ohbayashi and Sugiyama, 2018; Sáez-Vásquez and Delseny, 2019).

A linkage between root epidermal cell specification and ribosome biogenesis was first discovered through analysis of the RBF gene *ADENOSINE DIMETHYL TRANSFERASE1A* (*DIM1A*; Wieckowski and Schiefelbein, 2012). The DIM1A protein participates in *N*-6 dimethylation of the A1785 and A1786 bases in 18S rRNA (Wieckowski and Schiefelbein, 2012). The *dim1a* mutant exhibits ~20% reduction in the number of root hair cells due to an early cell fate switch that leads to ectopic non-hair cell formation (Wieckowski and Schiefelbein, 2012). However, the molecular mechanism underlying this cell fate switch was not determined.

In this study, we identified a nonsense allele of the RBF gene *ARABIDOPSIS PUMILIO23* (*APUM23*), designated as *apum23-4*. We discovered a significant reduction in root hair formation in *apum23-4* resulting from a cell fate switch mediated by abnormal upregulation of *MYB23*. Interestingly, we found that the increased *MYB23* expression in the *apum23-4* root epidermis was independent of the WER-GL3/EGL3-TTG1 complex but instead required ANAC082. We also found that other RBF mutants, including *dim1a*, exhibited a MYB23- and/or ANAC082-dependent root epidermal cell fate switch. Altogether, this study provides evidence for a novel regulatory pathway responsible for altering root epidermal cell fate in response to ribosomal defects.

RESULTS

Identification of the *apum23-4* Mutant

The *cpc-1* mutant produces ~30% of the normal number of root hair cells, due to 70% of H-position cells adopting the non-hair cell fate (Figures 1A and 1B). We took advantage of this intermediate phenotype and performed a *cpc-1* enhancer screen to identify genes involved in root epidermis specification. One of the resulting lines, later designated as *cpc-1 apum23-4*, exhibited an enhanced phenotype relative to *cpc-1*, producing almost hairless roots

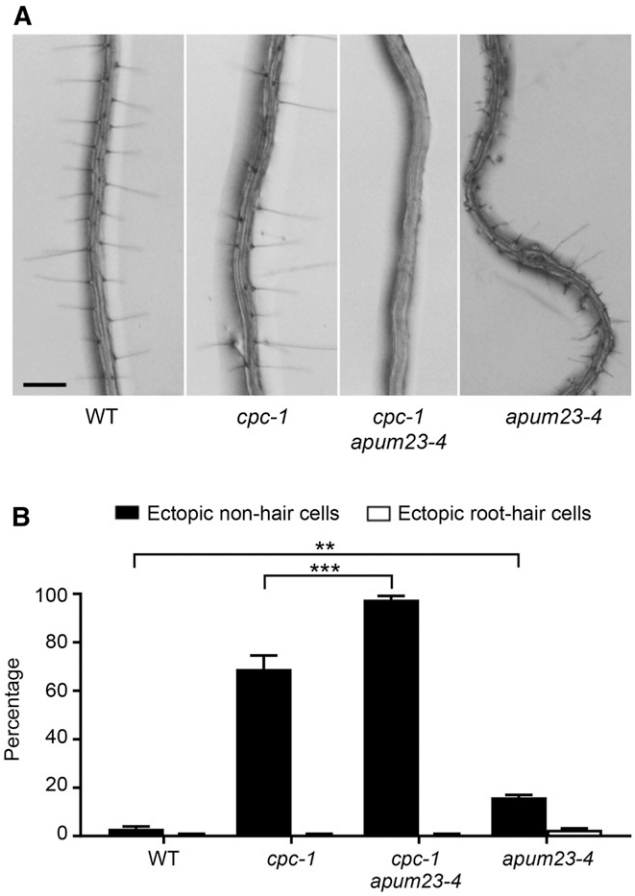

Figure 1. *The apum23-4* Mutation Enhances the *cpc-1* Mutant Phenotype.

(A) Root hair phenotypes of seedling roots of the wild type (WT), *cpc-1*, *cpc-1 apum23-4*, and *apum23-4*. Bar = 200 μm.

(B) Quantification of root epidermal cell specification in seedling roots of the wild type (WT), *cpc-1*, *cpc-1 apum23-4*, and *apum23-4*. Error bars indicate SDs from three replicates. Statistical significance was determined by one-way ANOVA. ***, $P < 0.001$; **, $P < 0.01$.

(Figures 1A and 1B). We isolated plants homozygous for the *apum23-4* single mutant and observed several growth abnormalities including delayed seed germination and shorter root hairs (Figure 1A; Supplemental Figure 1). However, the overall root architecture of the *apum23-4* mutant is comparable with that of the wild type (Supplemental Figure 2). Furthermore, quantification of root epidermal cell specification in *apum23-4* showed that 17% of the H-position cells failed to produce any surface protrusions, neither root hairs nor initial root hair bulges (i.e., 17% ectopic non-hair cells; see Methods; Figure 1B).

To identify the mutated gene in the *apum23-4* line, we performed map-based cloning and discovered a C-to-T single-nucleotide substitution within the first exon of the *AT1G72320* gene, which changes the 80th codon from CAG (Glu) to TAG (stop codon; Figure 2A). The *AT1G72320* gene is named *APUM23* and encodes an RNA binding protein from the Pumilio family (Murata and Wharton, 1995). Pumilio proteins are found in all eukaryotes and defined by the presence of tandem arranged, RNA-

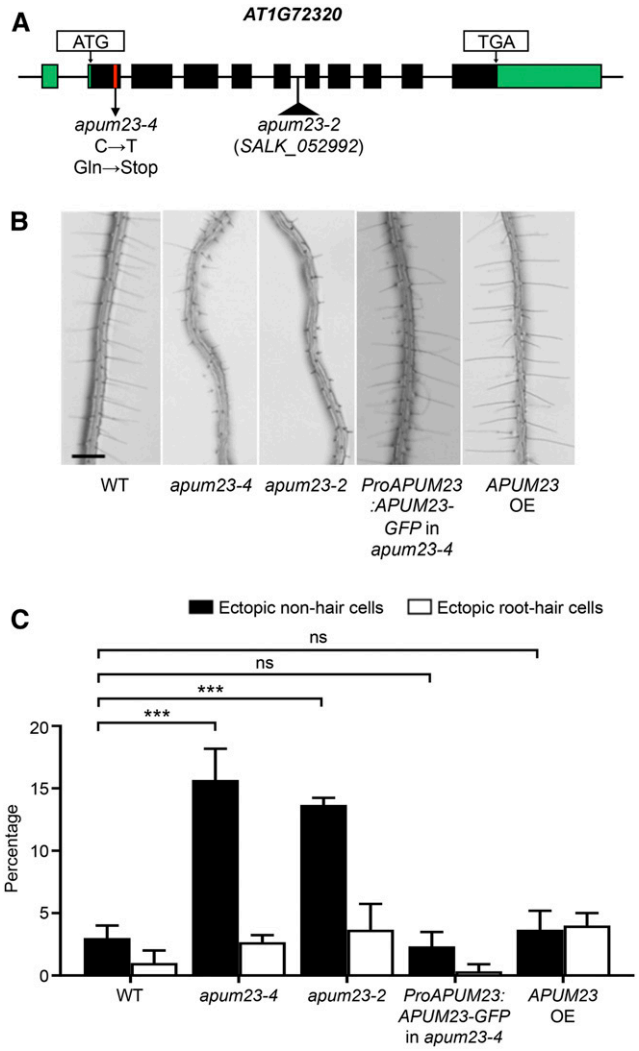

Figure 2. The *apum23-4* Mutant Possesses a Nonsense Mutation in the *APUM23* Gene.

(A) Schematic drawing of the *APUM23* (*AT1G72320*) gene, indicating the position of the mutated nucleotide in the *apum23-4* mutant. The green boxes indicate 5′ and 3′ UTRs, the black boxes indicate exons, and the black lines indicate introns. The single-base substitution in *apum23-4* is indicated by the red line. The position of the T-DNA insertion in the *apum23-2* (*SALK_052992*) mutant is indicated by the black triangle.

(B) Root hair phenotypes of seedling roots of the wild type (WT), *apum23-4*, *apum23-2*, *apum23-4* transformed with the *ProAPUM23*:*APUM23-GFP* transgene, and *apum23-4* transformed with the *Pro35S*:*APUM23-YFP* transgene (*APUM23* overexpression [OE]). Bar = 200 μm.

(C) Quantification of root epidermal cell specification in seedling roots of the wild type, *apum23-4*, *apum23-2*, *apum23-4* transformed with the *ProAPUM23*:*APUM23-GFP* transgene, and *APUM23* overexpression (OE). Error bars represent SDs from three replicates. Statistical significance was determined by one-way ANOVA. ns, not significant; ***, $P < 0.001$.

recognizing Pumilio and FBF homology (PUF) repeats (Zamore et al., 1997; Edwards et al., 2001), which number from 2 to 11 in members of the Arabidopsis Pumilio family (Francischini and Quaggio, 2009; Tam et al., 2010). Distinct from the canonical Pumilio proteins that mediate translational regulation largely through binding to the 3′ untranslated region (UTR) of mRNAs (Wickens et al., 2002; Szostak and Gebaue, 2013; Wang et al., 2018), APUM23, like its well-studied putative yeast (*Saccharomyces cerevisiae*) ortholog NOP9 (Thomson et al., 2007; Zhang et al., 2016), binds to rRNAs and contributes to pre-rRNA processing (Abbasi et al., 2010; Zhang and Muench, 2015).

Given that three mutant alleles of *APUM23* have been reported by Abbasi et al. (2010) and Huang et al. (2014), the allele identified in our study was designated as *apum23-4*. Other *APUM23* mutants were reported to exhibit delayed germination and slower growth (Abbasi et al., 2010; Huang et al., 2014), but no root epidermis analyses were performed. To determine whether the abnormal root epidermal cell specification in *apum23-4* was due to the *APUM23* mutation, we examined *apum23-2* mutant roots and discovered a comparable proportion of ectopic non-hair cells as in *apum23-4* (Figures 2A to 2C). We also generated a *ProAPUM23*:*APUM23-GFP* transgene containing the *APUM23* genomic sequence (including the native promoter) with an in-frame C-terminal GFP tag and introduced this into *apum23-4* plants. The resulting transformed plants exhibited the fully restored wild-type root hair length and root epidermal cell pattern (Figures 2B and 2C). These results confirm that the abnormal root epidermal phenotypes in *apum23-4* are due to the mutation in the *APUM23* gene.

We also performed an *APUM23* overexpression analysis by transforming *apum23-4* plants with a *Pro35S*:*APUM23-YFP* transgene. We observed a wild-type root hair length and root epidermal cell pattern in these transformed plants (Figures 2B and 2C), suggesting that a particular level or cellular distribution of the APUM23 protein is not critical for its role in root epidermal cell specification.

APUM23 Localizes in the Nucleoli of Multiple Root Tissues

To study the accumulation pattern of APUM23, we analyzed the *ProAPUM23*:*APUM23-GFP* transgenic plants and discovered APUM23-GFP accumulation in multiple tissues of the developing root (Figure 3A). In the root epidermis, the APUM23-GFP protein accumulated in both H- and N-position cells (Figure 3C).

To study the subcellular localization of APUM23, we first generated control transgenic plants bearing the mcherry-tagged FIBRILLARIN1 (FIB1) driven by its native promoter (*ProFIB1*:*FIB1-mcherry*). FIB1 is a known nucleolar protein participating in pre-rRNA and small nucleolar RNA processing (Pih et al., 2000; Pontvianne et al., 2010; Kalinina et al., 2018). Using 4′,6-diamidino-2-phenylindole (DAPI) staining to distinguish the nucleolus from the nucleoplasm, we verified the nucleolar localization of FIB1-mcherry in root epidermal cells (Figure 3B). We then generated plants bearing both the *ProAPUM23*:*APUM23-GFP* and *ProFIB1*:*FIB1-mcherry* transgenes, and we observed colocalization of the APUM23-GFP and FIB1-mcherry signals within individual root epidermal cells, indicating the nucleolar localization of APUM23 (Figure 3C).

Detailed examination of APUM23-GFP and FIB1-mcherry accumulation revealed notable features of nucleoli in the developing root epidermis. First, the relative nucleolar size in N-position cells appeared to decrease as cells aged. The N-position nucleoli were

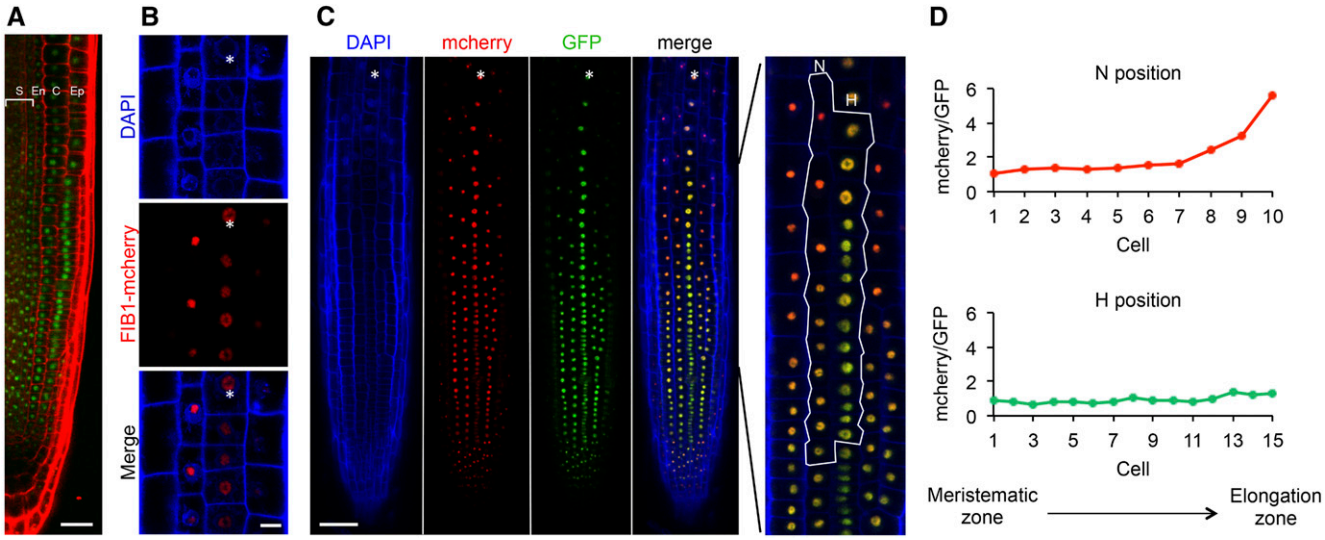

Figure 3. APUM23 Localizes to Nucleoli in Multiple Root Tissues.

(A) Accumulation of APUM23-GFP (green) in tissues of the *ProAPUM23*:*APUM23-GFP* root. Red represents PI staining for cell boundary visualization. Bar = 25 μm. C, cortex; En, endodermis; Ep, epidermis; S, stele.
(B) Overlay of DAPI staining (blue) and *ProFIB1*:*FIB1-mcherry* signals (red) in the root epidermis. Stars indicate H-position cell files. Bar = 10 μm.
(C) Overlay of DAPI staining (blue), *ProFIB1*:*FIB1-mcherry* (red), and *ProAPUM23*:*APUM23-GFP* (green) in the root epidermis (enlarged portion of the merged image is shown on the right with a non-hair cell file [N] and a hair cell file [H] outlined). Stars indicate H-position cell files. Compared to **(B)**, the root in **(C)** was only briefly stained with DAPI to enable visualization of cell boundaries. Bar = 50 μm.
(D) Quantification of the ratio of *ProFIB1*:*FIB1*-mcherry signals and *ProAPUM23*:*APUM23-GFP* signals within root epidermal cells in **(C)**. H- and N-Position cells used for quantification are outlined in white.

of similar size to H-position nucleoli in early meristematic cells, but their relative size decreased in older elongating cells (Figure 3C; Supplemental Figure 3). Second, the ratio between the FIB1-mcherry and APUM23-GFP proteins appeared to increase in N-position cells compared to H-position cells as they aged. The mcherry/GFP signal ratios were comparable between H- and N-position cells in the meristematic zone but diverged in the elongation zone (Figure 3D; Supplemental Figure 3). These observations suggest distinct nucleolar activities between root hair cells and non-hair cells during root epidermis development.

MYB23 Mediates Ectopic Non-Hair Cell Specification in *apum23-4*

To uncover the mechanisms underlying ectopic non-hair cell formation in the *apum23-4* mutant, we first made use of the *ProGL2*:*GUS* transcriptional reporter, a marker for early non-hair cell fate establishment (Masucci et al., 1996). In the wild-type roots, *ProGL2*:*GUS* exhibited strong preferential expression in N-position cells, while in *apum23-4* roots, ectopic *GL2* expression was observed in some H-position cells (Figure 4A). Specifically, ~15% of H-position cells expressed *ProGL2*:*GUS* signals in *apum23-4* (Figure 4E), a proportion comparable that of the ectopic non-hair cells in *apum23-4* (Figure 1B). Additionally, the ectopic non-hair cell formation in *apum23-4* is *GL2* dependent, given that the *gl2-1 apum23-4* double mutant lacked all non-hair cells in both H and N positions (Figure 4B). *GL2* has been reported to specify the non-hair cell fate during early cell differentiation by directly repressing multiple root hair transcription factor genes (Ohashi et al., 2003; Lin et al., 2015). Therefore, we conclude that the reduction in root hair cells in the H position of the *apum23-4* root epidermis is due to a *GL2*-dependent cell fate switch from root hair cells to non-hair cells.

GL2 expression in the root epidermis is controlled by a MYB-bHLH-WD40 complex consisting of WER, GL3/EGL3, and TTG1, and the absence of any of these three components leads to loss of both *GL2* expression and non-hair cells (Figures 4A and 4B; Galway et al., 1994; Lee and Schiefelbein, 2002; Bernhardt et al., 2003). To analyze the role of these components for the ectopic *GL2* expression in *apum23-4*, we separately introduced *wer-1*, *gl3 egl3*, and *ttg1* mutations into the *apum23-4 ProGL2*:*GUS* line. The *gl3 egl3 apum23-4* and *ttg1 apum23-4* mutants lacked significant *ProGL2*:*GUS* expression in the developing root epidermis (Figure 4A) and produced nearly 100% root hair cells in both the H and N positions (Figure 4B). However, the *wer-1 apum23-4* double mutant exhibited considerable *ProGL2*:*GUS* expression that greatly exceeded the *wer-1* single mutant (Figure 4A). Interestingly, the *ProGL2*:*GUS* signals in *wer-1 apum23-4* lacked N-position specificity (~20% of H-position cells and 31% of N-position cells expressed *ProGL2*:*GUS*; Supplemental Figure 4) and initiated accumulation in older cells (relative to the wild type; Figure 4A). Consistent with its *ProGL2*:*GUS* expression pattern, the *wer-1 apum23-4* mutant produced ~20 and 35% non-hair cells in the H and N positions, respectively (Figure 4B).

The results described above suggest that GL3/EGL3 and TTG1 are required, while WER is not required, for the ectopic non-hair

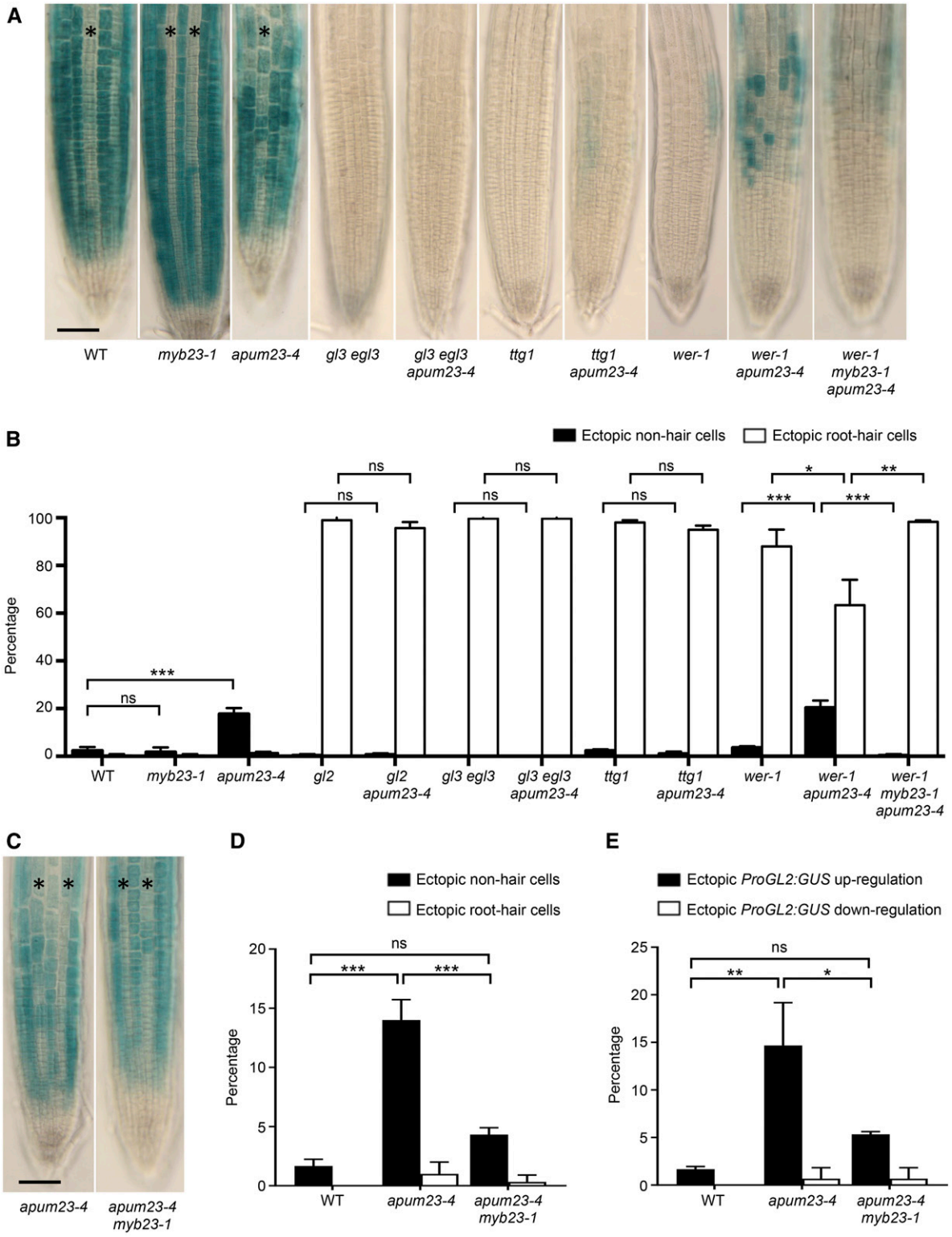

Figure 4. MYB23 Mediates Ectopic Non-Hair Cell Fate in the *apum23-4* Mutant through Upregulating *GL2*.

(A) Expression of *ProGL2:GUS* in seedling root tips of wild type (WT) and various mutant plants. Stars indicate H-position cell files. Bar = 50 μm.
(B) Quantification of epidermal cell specification in seedling roots of wild-type (WT) and mutant plants. Error bars represent SDs of three replicates. Statistical significance was determined by one-way ANOVA. ns, not significant; ***, $P < 0.001$; **, $P < 0.01$; *, $P < 0.05$.

cell formation in *apum23-4*. Therefore, we hypothesized that (an) other MYB protein(s) functions in place of WER in the *apum23-4* background to form a MYB-bHLH-WD40 complex and induce *GL2* expression to generate non-hair cells. MYB23 was a candidate for this role given its known root epidermis expression and close functional relationship to WER, although the *myb23-1* single mutant had no significant defects in root epidermal cell patterning (Kang et al., 2009). We introduced the *myb23-1* mutation into the *wer-1 apum23-4* background and discovered that the resulting triple mutant lacked *ProGL2*:*GUS* expression and essentially lacked non-hair cells (Figures 4A and 4B). Furthermore, we generated the *apum23-4 myb23-1* double mutant and observed a significantly reduced proportion of ectopic non-hair cells and ectopic *ProGL2*:*GUS*-expressing cells, relative to the *apum23-1* single mutant (both reduced to <5%; Figures 4C to 4E). Therefore, MYB23 is required for the ectopic *GL2* expression and non-hair cell fate specification in the *apum23-4* mutant.

Abnormal MYB23 Expression in *apum23-4*

In the wild-type roots, *MYB23* is preferentially expressed in the N-position cells of the developing root epidermis (Kang et al., 2009). To examine its expression in *apum23-4*, we used the *ProMYB23*:*GUS* reporter (Kang et al., 2009) and observed considerable ectopic β-glucuronidase (GUS) expression in the H-position cells compared to the wild type (Figure 5A). Specifically, 13% of the H-position cells in *apum23-4* showed detectable GUS signals (Supplemental Figure 5), a proportion comparable to that of ectopic non-hair cells in *apum23-4* (Figure 1B).

In the wild-type root epidermis, *MYB23* transcription is directly induced by the WER-GL3/EGL3-TTG1 complex, and loss of *WER* gene function eliminates *MYB23* expression (Figure 5A; Kang et al., 2009). However, we observed substantial *ProMYB23*:*GUS* expression in *wer-1 apum23-4*, and these *GUS* signals lacked N-position specificity (Figure 5A), which resembled the expression of *ProGL2*:*GUS* in *wer-1 apum23-4* (Figure 4A).

To test whether the observed ectopic *MYB23* expression leads to ectopic MYB23 protein accumulation, we made use of a *ProMYB23*:*MYB23-GFP* translational reporter (Kang et al., 2009). We discovered that MYB23-GFP protein accumulated ectopically in the nuclei of H-position cells of *apum23-4* as well as in both H- and N-position cells of *wer-1 apum23-4* (Figure 5B), which was consistent with the *ProMYB23*:*GUS* results (Figure 5A). Next, to determine whether these MYB23-GFP–accumulating cells are also expressing *GL2*, we examined the roots of *apum23-4* and *wer-1 apum23-4* plants bearing both the *ProMYB23*:*MYB23-GFP* and *ProGL2*:*GUS* reporters. In both the *apum23-4* and *wer-1 apum23-4* lines, we observed a correspondence between MYB23-GFP accumulation and *ProGL2*:*GUS* expression within individual root epidermal cells (Figure 5C). Additionally, we generated *apum23-4* plants bearing both the *ProGL3*:*GL3-YFP* (Bernhardt et al., 2005) and *ProGL2*:*GUS* reporters, and we found a similar correspondence between these two reporter signals in root epidermal cells (Figure 5D), supporting the notion that MYB23 induces *GL2* expression through its association with GL3.

In summary, we demonstrated a spatial correspondence between MYB23 accumulation and *GL2* expression in *apum23-4*, suggesting that *MYB23* upregulation in *apum23-4* causes abnormal spatial expression of *GL2* and, ultimately, ectopic non-hair cells. More importantly, our finding that ectopic *MYB23* expression in *apum23-4* is WER independent suggests a novel mechanism for upregulating *MYB23* in the *apum23-4* background.

ANAC082 Is Required for MYB23-Mediated Ectopic Non-Hair Cell Specification in *apum23-4*

Recently, the NAC family member ANAC082 was identified as a plant-specific mediator of ribosomal stress responses, given that the *anac082-1* mutant markedly reversed several developmental abnormalities in RBF mutants (Ohbayashi et al., 2017). Therefore, we sought to test whether the ectopic non-hair cells in *apum23-4* are ANAC082 dependent.

First, we generated the *anac082-1 apum23-4* double mutant and observed substantial recovery of the seed germination and growth rate compared to *apum23-4* (Supplemental Figure 1), indicating that these phenotypes are ANAC082 dependent. Furthermore, *anac082-1 apum23-4* produced <3% ectopic non-hair cells, which is comparable to the wild type (Figure 6B). This result was confirmed using a different *anac082* mutant (a T-DNA insertion mutation, *GABI_282H08*), which also reversed the *apum23-4* root hair pattern (Supplemental Figure 6A). Consistent with these observations, <3% of the H-position cells in *anac082-1 apum23-4* expressed the *ProGL2*:*GUS* reporter (Figure 6A; Supplemental Figure 6B). In addition, we found that the *anac082-1 wer-1 apum23-4* triple mutant restored the *wer-1* mutant phenotype, essentially lacking *ProGL2*:*GUS* expression in the root epidermis and producing >95% root hair cells in both H- and N-epidermis positions (Figures 6A and 6B). Notably, we observed no effect of the *anac082-1* or *GABI_282H08* mutant alone on root epidermis development; each single mutant exhibited a wild-type pattern of root epidermal cell types and *ProGL2*:*GUS* expression (Figures 6A and 6B; Supplemental Figure 6A). Therefore, ANAC082 has no significant role in root epidermal cell patterning under normal ribosome biogenesis conditions but mediates ectopic non-hair cell specification in the *apum23-4* background.

Figure 4. (continued).

(C) Expression of *ProGL2*:*GUS* in seedling root tips of *apum23-4* and *apum23-4 myb23-1* plants. Stars indicate H-position cell files. Bar = 50 μm.

(D) Quantification of epidermal cell specification in seedling roots of wild-type (WT), *apum23-4*, and *apum23-4 myb23-1* plants. Error bars represent SDs of three replicates. Statistical significance was determined by one-way ANOVA. ns, not significant; ***, $P < 0.001$.

(E) Quantification of *ProGL2*:*GUS* signals in seedling root tips of wild-type (WT), *apum23-4*, and *apum23-4 myb23-1* plants. Ectopic *ProGL2*:*GUS* upregulation refers to H-position cells exhibiting *ProGL2*:*GUS* expression, and ectopic *ProGL2*:*GUS* downregulation refers to N-position cells lacking *ProGL2*:*GUS* expression. Error bars represent SDs of three replicates. Statistical significance was determined by one-way ANOVA. ns, not significant; **, $P < 0.01$; *, $P < 0.05$.

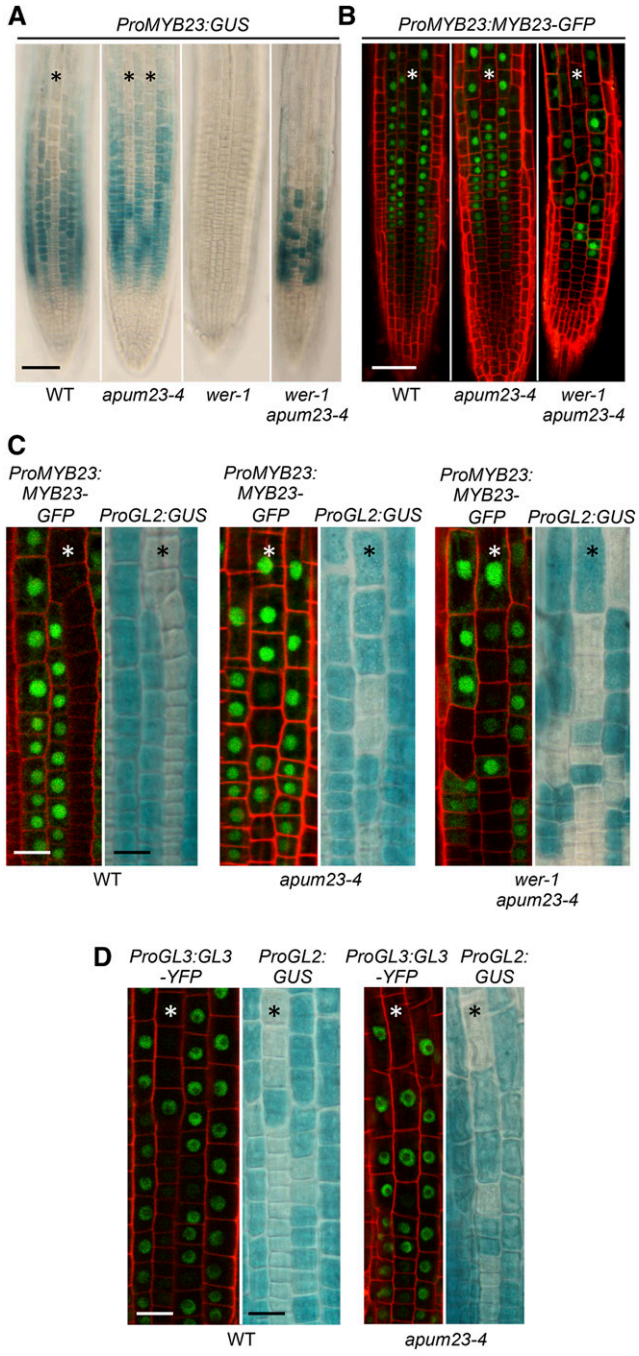

Figure 5. *apum23-4* Mutant Exhibits Ectopic *MYB23* Gene Expression.

(A) Expression of *ProMYB23*:*GUS* in the seedling root epidermis of the wild type (WT), *apum23-4*, *wer-1*, and *wer-1 apum23-4*. Stars indicate H-position cell files. Bar = 50 μm.

(B) Expression of *ProMYB23*:*MYB23-GFP* in the seedling root epidermis of the wild type (WT), *apum23-4*, and *wer-1 apum23-4*. Red represents PI staining and green represents MYB23-GFP signal. Stars indicate H-position cell files. Bar = 50 μm.

(C) Expression of *ProMYB23*:*MYB23-GFP* (left in each panel) and *ProGL2*:*GUS* (right in each panel) in one single seedling root tip of the wild type (WT), *apum23-4*, and *wer-1 apum23-4*. Stars indicate H-position cell files. Bar = 20 μm.

(D) Expression of *ProGL3*:*GL3-YFP* (left in each panel) and *ProGL2*:*GUS* (right in each panel) in one single seedling root tip of the wild type (WT) and *apum23-4*. Stars indicate H-position cell files. Bar = 20 μm.

Given that both ANAC082 and MYB23 are required for ectopic *GL2* expression and ectopic non-hair cell production in *apum23-4*, we examined the possible regulatory relationship between MYB23 and ANAC082. First, we examined *ProMYB23*:*GUS* expression in *anac082-1 apum23-4* and discovered that the ectopic *MYB23* expression in the H-position cells of *apum23-4* is ANAC082 dependent (Figure 6C; Supplemental Figure 6C). Similarly, the substantial *ProMYB23*:*GUS* expression in the *wer-1 apum23-4* mutant was found to be *anac082-1* dependent (Figure 6C). Consistent with these results, the ectopic *ProMYB23*:*MYB23-GFP* signals in *apum23-4* and *wer-1 apum23-4* were depleted by the *anac082-1* mutation (Figure 6D). Notably, the *anac082-1* single mutant exhibited no effect on *MYB23* expression (Figure 6C). Taken together, these results suggest that ANAC082 induces *MYB23* expression to cause ectopic *GL2* expression and switch epidermal cell fate in the *apum23-4* mutant.

ANAC082 belongs to the NAC domain transcription factor family (Ooka et al., 2003) and has been reported to have transcriptional activity when expressed in yeast (Ohbayashi et al., 2017). To determine whether ANAC082 might directly activate the transcription of *MYB23*, we adopted a dual-luciferase reporter system to assess *MYB23* promoter activity by overexpressed ANAC082 in a tobacco (*Nicotiana tabacum*) transient expression system (Supplemental Figures 7A and 7B). We found no significant *MYB23* promoter activation by ANAC082, indicating that ANAC082 alone is not sufficient to induce *MYB23* expression in this system. This could be due to the lack of cofactors of ANAC082 or intermediate regulators between *ANAC082* and *MYB23*. Therefore, it remains to be determined whether ANAC082 mediates *MYB23* expression via direct or indirect regulation.

ANAC082 expression is reported to be elevated in root tissues of several RBF mutants (Ohbayashi et al., 2017). Moreover, microarray analyses indicate *ANAC082* upregulation in whole adult *apum23-4* plants (Abbasi et al., 2010). To test whether *ANAC082* is upregulated in *apum23-4* seedling root tips, we performed quantitative real-time PCR (Figure 7A). Indeed, *ANAC082* transcript accumulation was significantly greater in the root tips of *apum23-4* mutants than the wild-type plants.

Multiple RBF Mutants Exhibit Ectopic Non-Hair Cells

The *apum23-4* mutant phenotype analyzed in this study is reminiscent of *dim1a*, a previously reported RBF mutant exhibiting ectopic *ProGL2*:*GUS* expression (Figure 8A; Wieckowski and Schiefelbein, 2012). Furthermore, like *wer-1 apum23-4*, the *wer-1 dim1a* double mutant exhibited significant *ProGL2*:*GUS* expression and non-hair cells in both H- and N-cell positions (Figures 8A and 8B; Supplemental Figure 4; Wieckowski and Schiefelbein, 2012). To test whether MYB23 plays the same role in the *dim1a* phenotype as it does in *apum23-4*, we generated the *wer-1 myb23-1 dim1a* and *myb23-1 dim1a* mutants. The *wer-1*

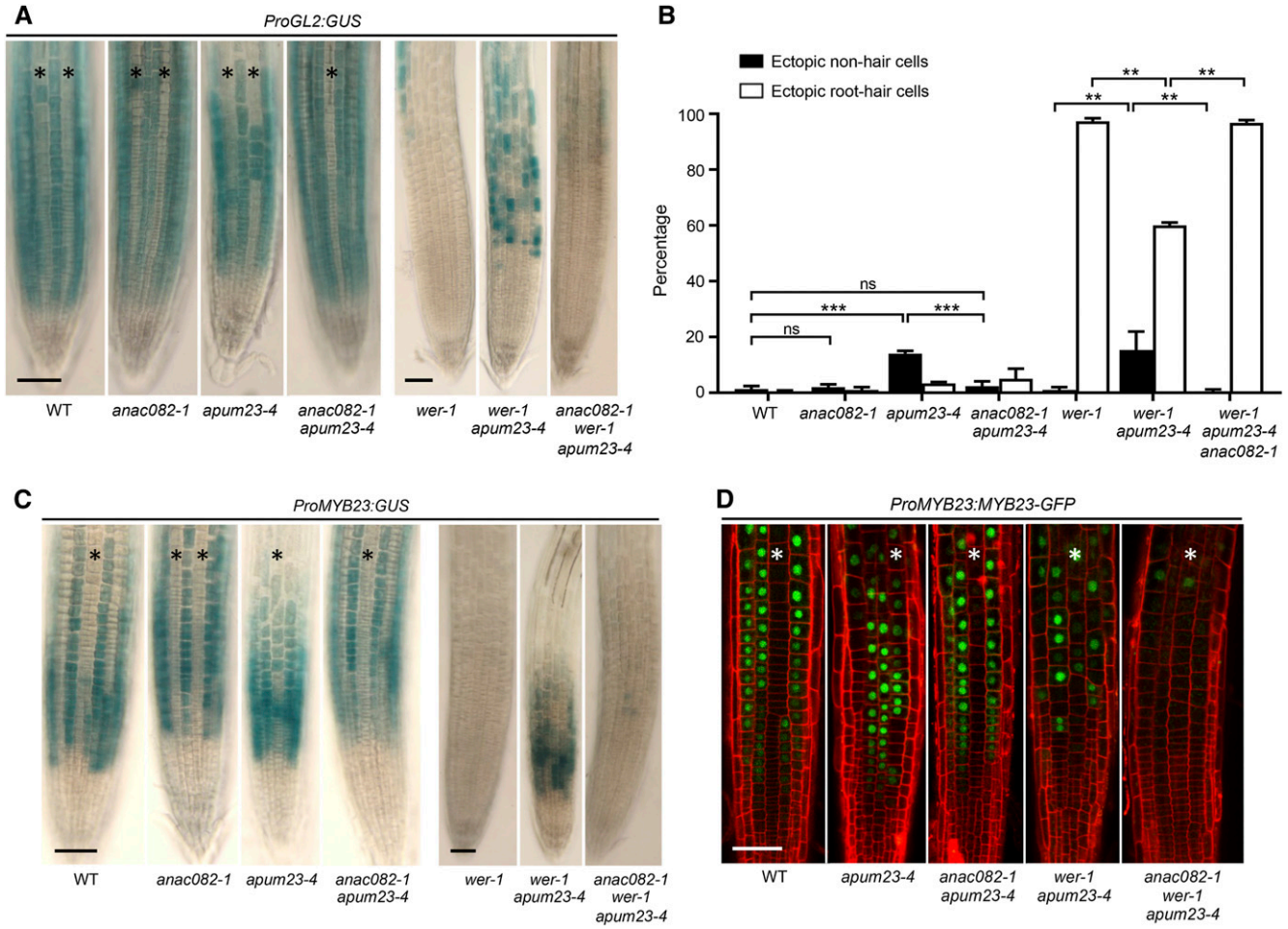

Figure 6. ANAC082 Is Required for Ectopic Non-Hair Cells in the *apum23-4* Mutant.

(A) Expression of *ProGL2*:*GUS* in the seedling root epidermis of the wild type (WT) and multiple mutants. Stars indicate H-position cell files. Bar = 50 μm.
(B) Quantification of root epidermal cell specification in the seedling roots of the wild type (WT) and multiple mutants. Error bars represent SDs from three replicates. Statistical significance was determined by one-way ANOVA. ns, not significant; ***, $P < 0.001$; **, $P < 0.01$.
(C) Expression of *ProMYB23*:*GUS* in the seedling root epidermis of the wild type (WT) and multiple mutants. Stars indicate H-position cell files. Bar = 50 μm.
(D) Expression of *ProMYB23*:*MYB23-GFP* in the seedling root epidermis of the wild type (WT) and multiple mutants. Red indicates propidium iodide staining and green indicates MYB23-GFP signals. Stars indicate H-position cell files. Bar = 50 μm.

myb23-1 dim1a triple mutant exhibited no significant *ProGL2*:*GUS* signals and ≥95% root hair cells in both H and N positions (Figures 8A and 8B), and the *myb23-1 dim1a* double mutant exhibited a significantly decreased proportion of ectopic non-hair cells compared to *dim1a* (Figure 8C). This shows that MYB23 is required for the ectopic non-hair cell formation in *dim1a*.

We also incorporated the *ProMYB23*:*GUS* reporter into the *dim1a* mutant and observed ectopic GUS signals in H-position cells at a frequency comparable to *apum23-4* (Figure 9A; Supplemental Figure 5). Furthermore, the *wer-1 dim1a* double mutant exhibited substantial *ProMYB23*:*GUS* signals (Figure 9A), indicating WER-independent *MYB23* upregulation similar to the *apum23-4* mutant.

Next, we tested the effect of ANAC082 on the *dim1a* phenotype. We introduced the *anac082-1* mutation into *dim1a* mutant lines carrying *ProMYB23*:*GUS* or *ProGL2*:*GUS* reporters and found that each reporter exhibited the wild-type expression pattern in the *dim1a anac082-1* background (Figures 9A and 9B; Supplemental Figures 6B and 6C). Consistently, both *dim1a anac082-1* and *dim1a GABI_282H08* mutants restored the wild-type root epidermal cell patterning (Figure 9C; Supplemental Figure 5A). In addition, *anac082-1* eliminated expression of the *ProMYB23*:*GUS* and *ProGL2*:*GUS* reporters, as well as non-hair cell production, in the *wer-1 dim1a* double mutant (Figures 9A to 9C). Taken together, these results show that ANAC082 plays a similar role of inducing MYB23-dependent *GL2* expression and cell fate switching in both the *dim1a* and *apum23-4* mutants.

Although the *apum23* and *dim1a* mutants exhibit similar root epidermis phenotypes, the APUM23 and DIM1A proteins have distinct biochemical functions in ribosome biogenesis. Accordingly, we hypothesized that the ectopic production of non-hair cells may be a general response to defective ribosome biogenesis.

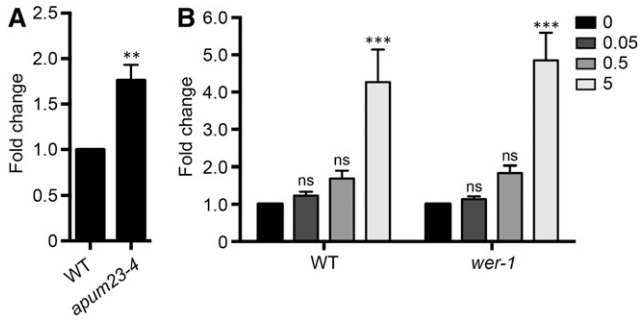

Figure 7. *ANAC082* Is Upregulated in *apum23-4* Mutant and CHX-Treated Seedling Roots.

(A) Relative amounts of *ANAC082* transcripts in root tips of the wild-type (WT) and *apum23-4* plants, determined by quantitative real-time PCR. Error bars indicate SDs from three replicates. Statistical significance was determined by *t* test. **, $P < 0.01$.

(B) Relative amounts of *ANAC082* transcripts in root tips of the wild-type (WT) and wer-1 plants treated with different concentrations of CHX (0, 0.05, 0.5, and 5 μg/mL). Error bars indicate SDs from three replicates. For both the wild type (WT) and *wer-1*, statistical significance between each CHX concentration and mock treatment (0 μg/mL) was determined by one-way ANOVA. ns, represents not significant; ***, $P < 0.001$.

To test this, we examined a collection of previously defined RBF mutants (Supplemental Table 1; Weis et al., 2015a). Among these, we discovered that mutations of the *PROTEIN ARGININE METHYLTRANSFERASE3* (*PRMT3*) gene, *prmt3-1* and *prmt3-2*, exhibited ectopic non-hair cells similar to *apum23-4* and *dim1a* (Figure 8B). The *prmt3-1* mutant also exhibited delayed germination (Supplemental Figure 1). During rRNA biogenesis, PRMT3 influences the balance between two alternative pre-rRNA processing pathways (Hang et al., 2014).

To study the cause for the ectopic non-hair cells in *prmt3-1*, we introduced the *ProGL2*:*GUS* reporter and found ~20% of the H-position cells exhibited ectopic *ProGL2*:*GUS* expression (Figure 8A; Supplemental Figure 8). Furthermore, the *wer-1 prmt3-1* double mutant exhibited substantial *ProGL2*:*GUS* expression and produced non-hair cells in both H and N positions, demonstrating a WER-independent effect (Figures 8A and 8B; Supplemental Figure 4). A role for MYB23 in the *prmt3-1* phenotype was shown by the elimination of *ProGL2*:*GUS* expression and non-hair cell production in the *wer-1 myb23-1 prmt3-1* plants, relative to the *wer-1 prmt3-1* double mutant (Figures 8A and 8B), and the significant decrease in ectopic non-hair cells in the *prmt3-1 myb23-1* double mutant compared to *prmt3-1* (Figure 8C). Finally, the *prmt-1* mutant exhibited a comparable proportion of H-position cells expressing *ProMYB23*:*GUS* as the *apum23-4* and *dim1a* (Figure 9A; Supplemental Figure 5). Therefore, like *apum23-4* and *dim1a*, the ectopic non-hair cell specification in *prmt3-1* is mediated by MYB23.

In summary, we identified two additional RBF mutants (*dim1a* and *prmt3-1*) exhibiting ectopic non-hair cells likely resulting from similar misregulation of epidermal cell fate as in *apum23-4*. These findings support the hypothesis that epidermal cell fate switching is a general response to ribosomal defects rather than a particular RBF deficiency.

CHX Treatment Induces WER-Independent *GL2* Expression

In addition to genetic disturbances in RBF genes, drug-induced ribosomal defects can also trigger ectopic establishment of non-hair cell fates. Cycloheximide (CHX), widely used as a translation inhibitor, disrupts pre-rRNA processing in yeast and mammals (de Kloet, 1966; Stoyanova and Hadjiolov, 1979). Interestingly, a treatment of 5 μg/mL CHX was reported to induce ectopic *GL2* expression in a significant portion of H-position cells in the wild-type root epidermis (Wieckowski and Schiefelbein, 2012), an effect similar to the RBF mutants. We further analyzed the effect of CHX treatment on root epidermis development by monitoring *ProGL2*:*GUS* expression in the *wer-1* mutant. Using a series of CHX concentrations, including 5 μg/mL, we found that *ProGL2*:*GUS* expression was induced in a *WER*-independent manner in both H- and N-position cells (Figure 10). Notably, the *wer-1 myb23-1* and *wer-1 anac082-1* double mutants exhibited no *ProGL2*:*GUS* upregulation in response to CHX treatments (Figure 10), implying that the effect of CHX also relies on the ANAC082-MYB23 regulatory module that operates in the RBF mutants.

We also used quantitative real-time PCR to determine whether *ANAC082* expression is elevated by CHX treatment (Figure 7B). Compared to the mock treatment (0 μg/mL), both 0.05 and 0.5 μg/mL CHX treatments caused slight *ANAC082* upregulation that was not statistically significant, whereas treatment with 5 μg/mL CHX caused significant *ANAC082* upregulation.

The *apum24-2* Mutant Is a Distinct Type of RBF Mutant with Ectopic Non-Hair Cells

Another Arabidopsis Pumilio protein, APUM24, has been identified as an RBF required for pre-rRNA processing (Shanmugam et al., 2017; Maekawa et al., 2018). As *APUM24* knockout mutants were reported to exhibit seed abortion due to defective female gametogenesis and embryogenesis, we analyzed the *APUM24* knockdown mutant *apum24-2* (Shanmugam et al., 2017; Maekawa et al., 2018). We discovered that *apum24-2* mutant roots exhibited shorter root hairs resembling other examined RBF mutants (Figure 11A). Furthermore, the *apum24-2* mutant produced a significant proportion of ectopic non-hair cells (Figure 11D) and ectopic *ProGL2*:*GUS* signals in the H position (Figure 11B; Supplemental Figure 8). Therefore, like *APUM23*, knockdown of the *APUM24* gene function leads to ectopic non-hair cell specification.

Structural studies of the APUM23 yeast ortholog Nop9 and the APUM24 human ortholog Puf-A revealed that the two proteins, although both containing 11 PUF repeats, possess divergent protein structures and nucleotide binding characteristics (Qiu et al., 2014; Zhang et al., 2016). To test the functional relationship between the Arabidopsis APUM23 and APUM24 proteins, we created a *ProAPUM23*:*APUM24* transgene and transformed it into the *apum23-4* mutant, and reciprocally, we created a *ProAPUM24*:*APUM23* transgene and transformed it into the *apum24-2* mutant. In each case, the resulting transgenic plants exhibited the abnormal root epidermis phenotypes of the original mutant backgrounds (Figure 11D), indicating that APUM23 and APUM24 are functionally distinct.

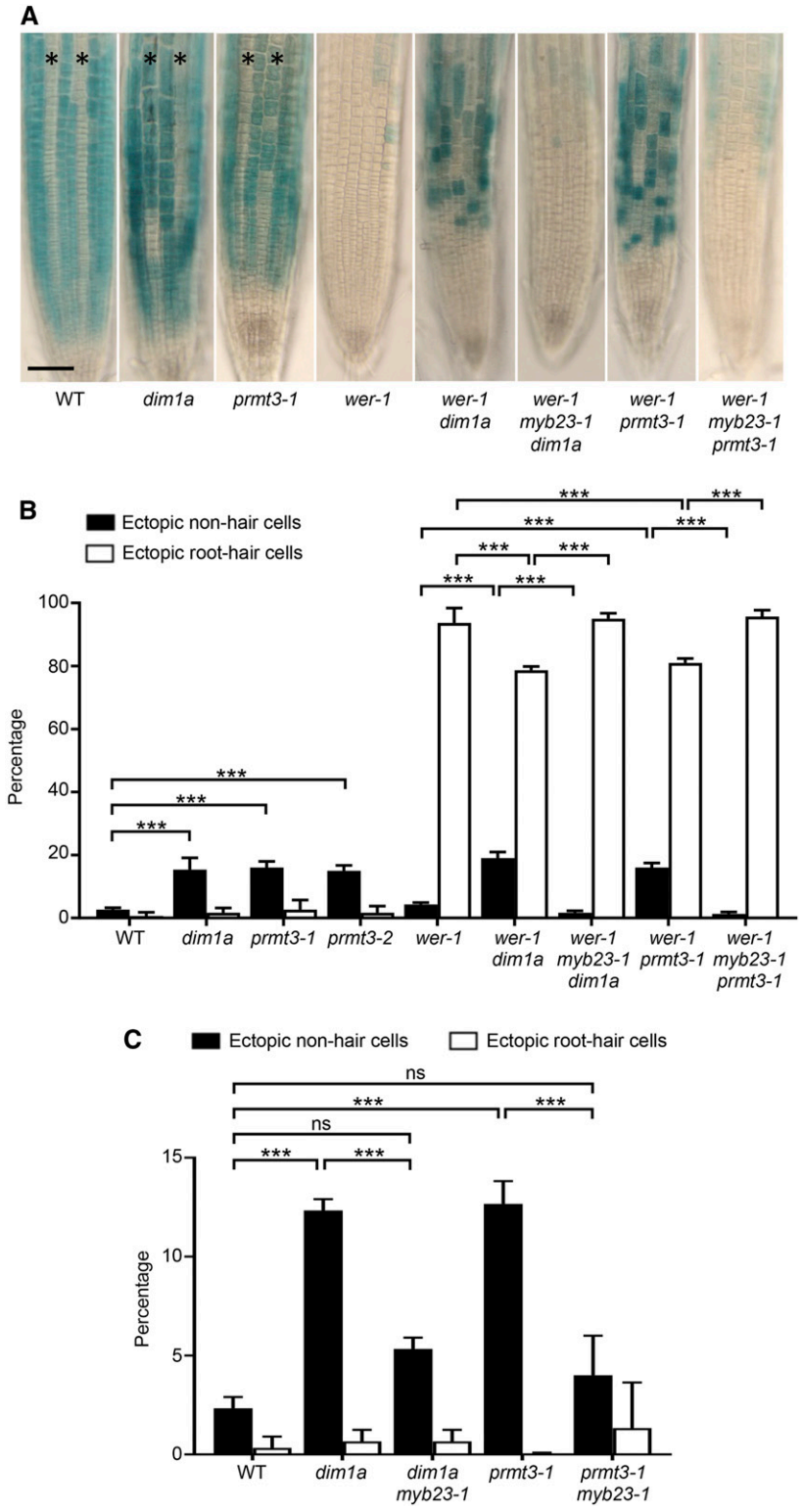

Figure 8. *dim1a* and *prmt3-1* Mutants Exhibit MYB23-Dependent Ectopic Non-Hair Cell Fate Specification.

(A) Expression of *ProGL2*:*GUS* in the seedling root epidermis of the wild type (WT) and multiple mutants. Stars represent H-position cell files. Bar = 50 μm.
(B) Quantification of epidermal cell specification in seedling roots of the wild type (WT) and multiple mutants. Error bars represent SDs from three replicates. Statistical significance was determined by one-way ANOVA. ***, $P < 0.001$.

We then studied the cause for the ectopic non-hair cells in *apum24-2*. The *wer-1 apum24-2* double mutant exhibited no significant non-hair cells in the H position but a considerable proportion of non-hair cells (>30%) in the N position, and the *wer-1 myb23-1 apum24-2* mutant showed no significant reduction in the proportion of these non-hair cells (Figure 11E). Furthermore, the *apum24-2 myb23-1* mutant produced >10% ectopic non-hair cells, which is not significantly different from *apum24-2* (Figure 11D). In addition, the *ProMYB23*:*GUS* reporter showed dramatically decreased expression in the *apum24-2* root epidermis (Figure 11C). These results indicate that, unlike *apum23-4*, the ectopic non-hair cells in *apum24-2* are MYB23 independent. Consistent with this, the *apum23-4 apum24-2* double mutant produced an additive increase of ectopic non-hair cells compared to each of the two single mutants (Figure 11D), suggesting that ectopic non-hair cell production in *apum23-4* and *apum24-2* is due to separate pathways. Notably, the *gl3 egl3 apum24-2* mutant still efficiently depleted all non-hair cells in both H and N positions (Figure 11E). Therefore, the ectopic non-hair cells in the *apum24-2* mutant apparently still rely on formation of the MYB-bHLH-WD40 complex. Finally, we tested whether the ectopic non-hair cells in *apum24-2*, although independent of *MYB23*, still require *ANAC082*. Indeed, the *apum24-2 anac082-1* double mutant exhibited no significant ectopic non-hair cell production (Figure 11F), indicating that ANAC082 mediates ectopic non-hair formation in the *apum24-2* mutant.

Flagellin 22 Peptide Treatment Induces WER-Independent *GL2* Expression Mediated by MYB23 and ANAC082

This study revealed that genetic defects in ribosome biogenesis caused by RBF mutants trigger ANAC082-mediated *MYB23* expression that then induces *GL2* expression and non-hair cell fate establishment. To determine whether this regulatory pathway might be activated by other stresses, we first analyzed the effect of various stress conditions on *ANAC082* expression. Interestingly, several public microarray and RNA sequencing data sets indicate that plant pathogen treatments cause *ANAC082* upregulation in leaf tissues (Ferrari et al., 2007; Winter et al., 2007). To study whether biotic stresses and the resulting plant defense responses affect root epidermal cell specification, we used flagellin22 (flg22), a peptide corresponding to the conserved domain of bacterial flagellin (Gómez-Gómez et al., 1999), as a plant immune response elicitor. Treatment with 1 μM flg22 caused no significant alterations in root epidermal cell specification in wild-type roots (Figure 12A). However, *wer-1* mutants treated with 1 μM flg22 exhibited significant non-hair cell formation in the N position (Figure 12A). Furthermore, *ProGL2*:*GUS* expression was increased in the root epidermis of *wer-1* mutants treated with 1 μM flg22 (Figure 12B). To determine whether this effect of flg22 on *wer-1* is dependent on *ANAC082* or *MYB23*, we repeated the same treatment on the *wer-1 myb23-1* and *wer-1 anac082-1* double mutants. Interestingly, neither double mutants showed a significant increase in *ProGL2*:*GUS* expression or non-hair cell formation (Figures 12A and 12B). Therefore, flg22 treatment induces WER-independent *GL2* expression in the root epidermis that requires ANAC082 and MYB23, suggesting the activation of a regulatory pathway that overlaps with that induced by RBF mutants.

DISCUSSION

A Working Model for Cell Patterning in RBF Mutant Root Epidermis

In this study, we uncovered a regulatory mechanism mediating a cell fate switch in response to defective ribosome biogenesis. Based on our combined analysis of ribosome biogenesis mutants (*apum23-4*, *dim1a*, and *prmt3-1*) and CHX-treated plants that all produced ectopic non-hair cells, we determined that this cell fate switch is the result of aberrant induction of *MYB23* gene expression by the ribosomal stress response mediator ANAC082. Therefore, this work provides evidence for a molecular linkage between ribosomal status and cell fate specification in plants.

We suggest a model to explain our findings (Figure 13). During early development of the wild-type root epidermis, expression of the *GL2* and *MYB23* genes is induced by the WER-GL3/EGL3-TTG1 complex, which predominantly occurs in N-position cells and leads to non-hair cell fate specification (Figure 13A). The expression of *GL2* and *MYB23* is absent (or low) in the H-position cells due to SCM-dependent inhibition of *WER* expression and CPC-dependent inhibition of WER-GL3/EGL3-TTG1 complex formation, allowing for root hair cell differentiation in these cells. In *apum23-4* (and presumably *dim1a*, *prmt3-1*, and CHX-treated plants; Figure 13B), an ANAC082-dependent pathway is activated in response to impaired ribosome biogenesis. In addition to the WER-GL3/EGL3-TTG–induced *MYB23* expression in N-position cells, ANAC082 also generates *MYB23* expression in both H- and N-position cells via direct or indirect regulation. In the N-position cells, the additional *MYB23* expression further supports WER/MYB23-dependent gene regulation. In the H-position cells, the additional *MYB23* expression leads to elevated levels of MYB23/WER that, in some cells (~20%), is sufficient to overcome CPC inhibition and thereby induce *GL2* expression and ectopic non-hair cell specification. The other H-position cells might accumulate a level of MYB23 that is higher than normal but below the threshold required to achieve ectopic non-hair cell specification, and so they adopt the hair cell fate instead.

The Role of MYB23 in Response to Ribosome Biogenesis Defects

The MYB23 protein is most similar to two other Arabidopsis R2R3-type MYB transcription factors, WER and GL1, and it participates

Figure 8. (continued).

(C) Quantification of epidermal cell specification in seedling roots of the wild type (WT) and multiple mutants. Error bars represent SDs from three replicates. Statistical significance was determined by one-way ANOVA. ***, $P < 0.001$ and.

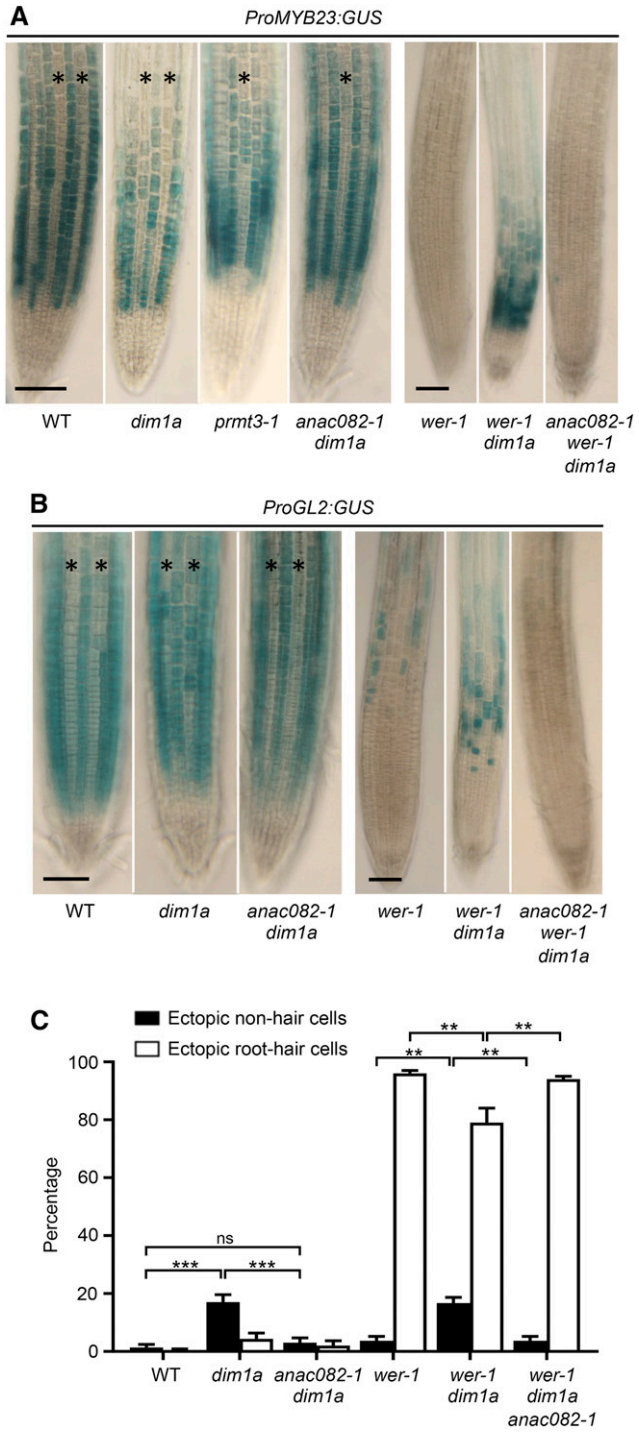

Figure 9. ANAC082 Is Required for Ectopic Non-Hair Cells in the *dim1a* Mutant.

(A) Expression of *ProMYB23*:*GUS* in the seedling root epidermis of wild type (WT) and multiple mutants. Stars indicate H-position cell files. Bar = 50 μm.

(B) Expression of *ProGL2*:*GUS* in the seedling root epidermis of the wild type (WT) and multiple mutants. Stars indicate H-position cell files. Bar = 50 μm.

with them to specify cell fates in the root epidermis and shoot epidermis. In the developing shoot epidermis, *MYB23* is required for proper trichome branching, and it acts redundantly with *GL1* to control trichome initiation (Kirik et al., 2005; Tominaga et al., 2007; Li et al., 2009; Balkunde et al., 2010). In the root epidermis, MYB23 acts redundantly with WER to generate the WER-GL3/EGL3-TTG1 complex responsible for non-hair cell fate specification, although the *myb23* single mutant exhibits no significant root epidermis defects (Kang et al., 2009). In this study, we expanded our knowledge of MYB23 function by showing that it mediates ectopic non-hair cell specification in response to defective ribosome biogenesis. Specifically, we showed that RBF mutants (*apum23-4*, *dim1a*, and *prmt3-1*) exhibited MYB23-dependent ectopic non-hair cell production (Figures 4 and 8), and CHX-treated *wer-1* roots exhibited MYB23-dependent *GL2* expression (Figure 10). It is notable that a functionally redundant player in root epidermis cell specification (MYB23) was recruited for this role, rather than the primary R2R3 MYB regulator (WER), suggesting that the evolution of regulatory pathways may take advantage of duplicate genes.

The plasticity of root epidermal cell specification under challenging conditions is well known. Ectopic non-hair cells can be induced by salt stress (Wang et al., 2008), while ectopic root hair cells can be induced by phosphate or iron deficiencies (Schmidt and Schikora, 2001; Müller and Schmidt, 2004). In this study, we report that ectopic non-hair cell formation is triggered by defects in ribosome biogenesis via activation of *MYB23*. Interestingly, our discovery is reminiscent of the role of ETC1 in inducing production of ectopic root hair cells upon phosphate deficiency (Rishmawi et al., 2018). Under normal growth conditions, ETC1 functions redundantly with CPC, and the *etc1* single mutant exhibits no defects in root epidermis cell patterning (Kirik et al., 2004; Simon et al., 2007). Thus, our study and the ETC1 study show that redundant regulators in the root epidermis cell fate network operate as stress-responding elements to modulate cell fates. Furthermore, these studies raise the possibility that additional regulators in the network may have similar unrecognized roles in controlling root epidermal cell fate in response to various plant stresses.

This study also has implications for our understanding of *MYB23* transcriptional regulation. A previous study identified WER binding sites in the *MYB23* promoter and showed that WER, GL3/EGL3, and TTG1 were necessary for *MYB23* transcription in the developing root epidermis (Kang et al., 2009). Our study showed that *MYB23* expression in the root epidermis is WER independent under conditions of impaired ribosome biogenesis and is instead mediated by ANAC082. It is notable that the ANAC082-dependent *MYB23* expression occurred in both H- and N-position cells and exhibited a later developmental start point within the distal meristematic zone (Figure 4). These features suggest a novel regulatory module that induces *MYB23* expression independent of positional cues and following a different developmental timeline. However, it remains unknown whether ANAC082, a potential

(C) Quantification of root epidermal cell specification in seedling roots of the wild type (WT) and multiple mutants. Error bars represent SDS from three replicates. Statistical significance was determined by one-way ANOVA. ns, not significant; ***, $P < 0.001$; **, $P < 0.01$.

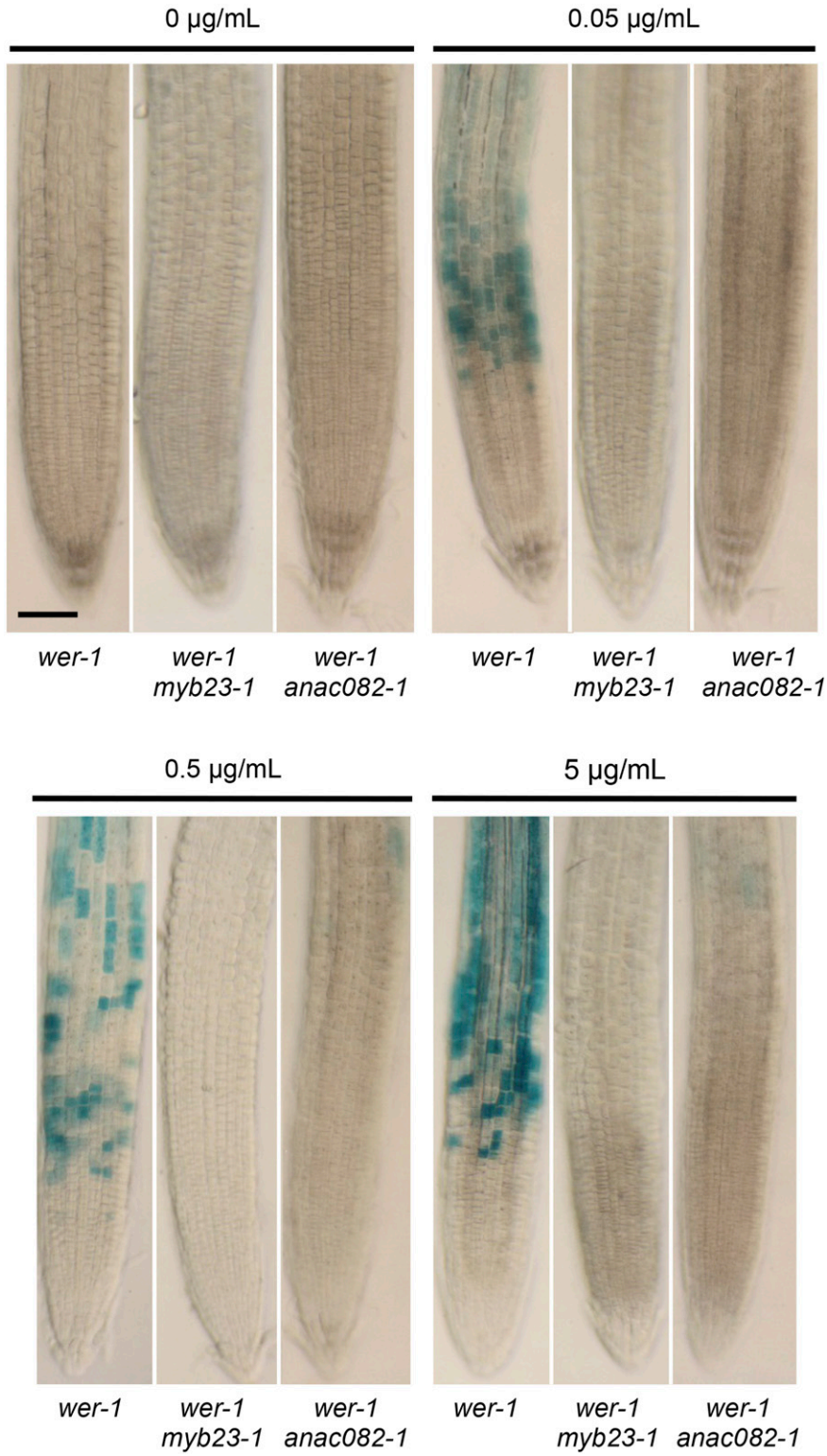

Figure 10. MYB23 and ANAC082 Mediate WER-Independent *GL2* Upregulation Triggered by CHX Treatment.

Expression of *ProGL2*:*GUS* in the root epidermis of *wer-1*, *wer-1 myb23-1*, and *wer-1 anac082-1* seedlings treated with a series of concentrations of CHX. Bar = 50 μm.

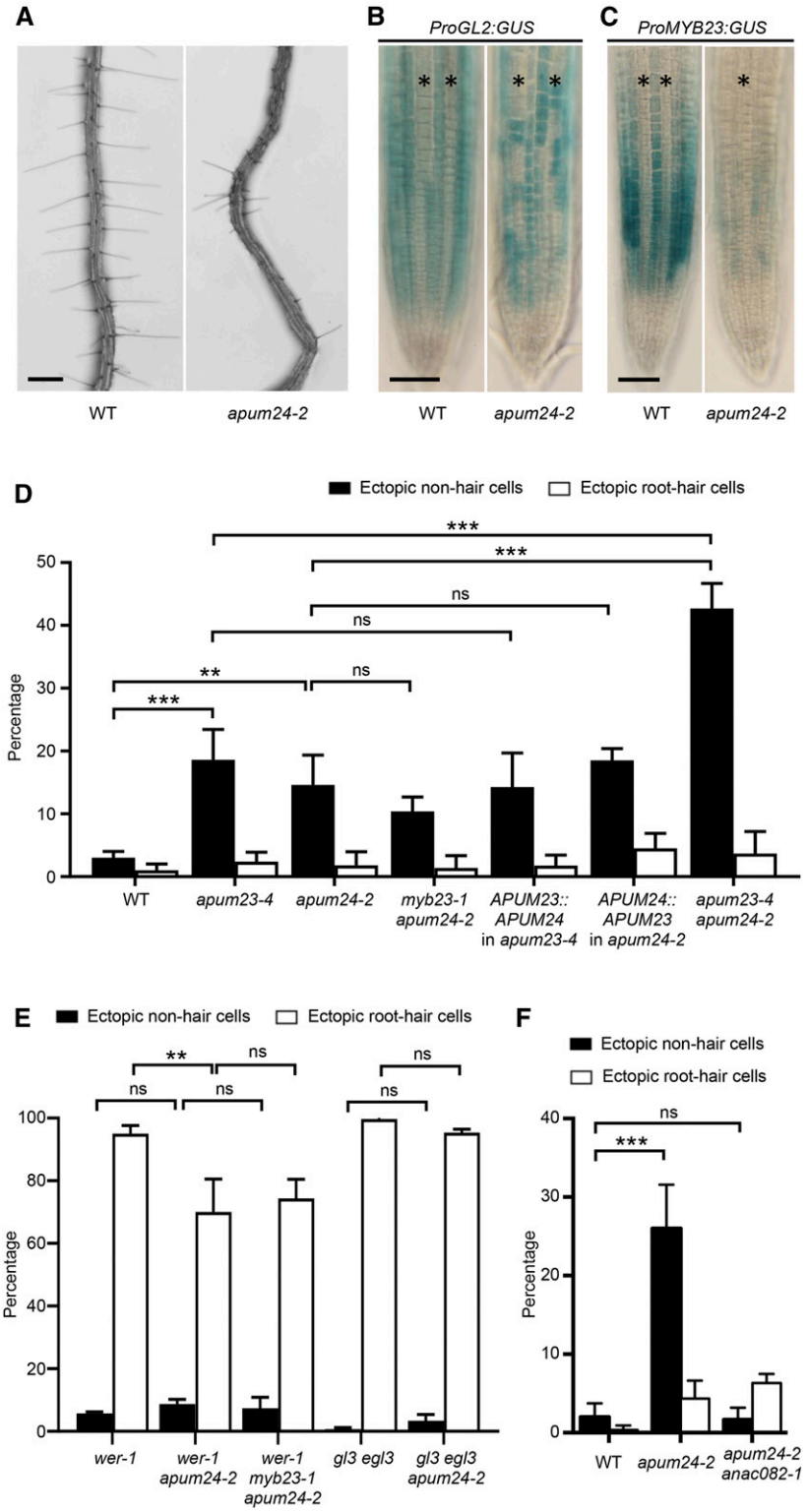

Figure 11. *apum24-2* Mutant Exhibits MYB23-Independent Ectopic Non-Hair Cell Production.

(A) Root hair phenotypes of the wild-type (WT) and *apum24-2* seedling roots. Bar = 200 μm.
(B) Expression of *ProGL2*:*GUS* in the seedling root epidermis of the wild type (WT) and *apum24-2*. Stars indicate H-position cell files. Bar = 50 μm.
(C) Expression of *ProMYB23*:*GUS* in the seedling root epidermis of the wild type (WT) and *apum24-2*. Stars indicate H-position cell files. Bar = 50 μm.

transcriptional activator (Yamaguchi et al., 2015; Ohbayashi et al., 2017), induces *MYB23* expression directly or indirectly. Our results using a transient dual-luciferase assay (Supplemental Figure 7) suggest that ANAC082 alone is not sufficient to activate *MYB23* expression. Therefore, it is likely that ANAC082 either indirectly upregulates *MYB23* expression by regulating some intermediate regulators or ANAC082 requires cofactors for *MYB23* promoter binding or transactivation. In this respect, it is interesting to note that the NAC domain has dimerization features (Ernst et al., 2004; Olsen et al., 2004) and that ANAC082 interacts with numerous NAC transcription factors, but not itself in vitro (Yamaguchi et al., 2015).

In a series of experiments, we showed that the *myb23-1* mutation largely reverses the ectopic non-hair cell defects in the *apum23-4*, *dim1a*, and *prmt3-1* mutants (Figures 4D, 4E, and C8C), indicating the essential role of MYB23 in establishing ectopic non-hair cell fate in these RBF mutants. Nevertheless, there remains a small proportion (~5%) of ectopic *GL2* expression and non-hair cells in these double mutants. By contrast, the introduction of the *anac082-1* mutation into the *apum23-4* and *dim1a* mutants essentially restored all root hair cells in the H positions (Figures 6B and 9C). These results suggest that MYB23 is the major, but not the only, regulator for the ectopic non-hair cell fates in RBF mutants that is induced by ANAC082. It is possible that other R2R3-type MYB proteins are also upregulated in an ANAC082-dependent manner and contribute to ectopic *GL2* expression together with MYB23.

Interestingly, among the RBF mutants we analyzed, the *apum24-2* mutant was unique in generating ectopic non-hair cells in a MYB23-independent manner. Specifically, the *myb23-1* mutation had no significant effect on non-hair cell specification in the *wer-1 apum24-2* or *apum24-2* mutants (Figure 11). However, these ectopic non-hair cells still require ANAC082 (Figure 11F). Thus, these findings suggest the existence of multiple regulatory mechanisms downstream of ANAC082 to mediate the effect of impaired ribosome biogenesis on root epidermal cell specification.

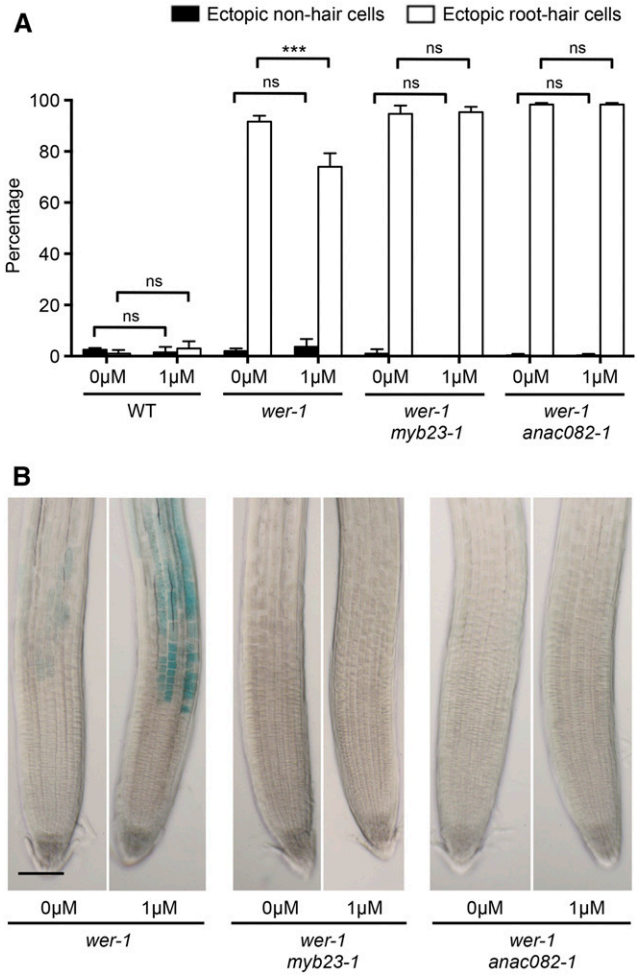

Figure 12. Flg22 Treatment Induces WER-Independent *GL2* Expression Mediated by ANAC082 and MYB23.

(A) Quantification of root epidermal cell specification in wild-type (WT), *wer-1*, *wer-1 myb23-1*, and *wer-1 anac082-1* seedling roots with 1 μM flg22 and without flg22 treatments. Error bars represent SDs from three replicates. Statistical significance was determined using one-way ANOVA. ns, not significant; ***, $P < 0.001$.

(B) *ProGL2:GUS* expression in *wer-1*, *wer-1 myb23-1*, and *wer-1 anac082-1* seedling roots with 1 μM flg22 and without flg22 treatments. Bar = 50 μm.

Ribosome Biogenesis and Plant Development

Ribosomes are necessary for protein synthesis, and developmental processes in general rely on efficient ribosome biogenesis. In plants, multiple studies have shown that mutants of functionally unrelated RBF genes exhibit similar alterations in cotyledon, leaf, and root development (Weis et al., 2015a; Sáez-Vásquez and Delseny, 2019). Accordingly, defective ribosome biogenesis of different origins appears to impact plant development through a common regulatory pathway (Byrne, 2009; Weis et al., 2015a). It is proposed that the ribosomal abnormalities in various RBF/RP mutants, including insufficient ribosome production and aberrant/unbalanced heterogeneity of ribosome

Figure 11. (continued).

(D) Quantification of root epidermal cell specification in wild-type (WT) and various mutant seedlings. Error bars represent SDs from three replicates. Statistical significance was determined by one-way ANOVA. ns, not significant; ***, $P < 0.001$; **, $P < 0.01$.

(E) Quantification of root epidermal cell specification in seedling roots of multiple mutants. Error bars represent SDs from three experiments. Statistical significance was determined by one-way ANOVA. ns, not significant. **, $P < 0.01$.

(F) Quantification of root epidermal cell specification in seedling roots of wild type (WT), *apum24-2*, and *apum24-2 anac082-1* mutants. Error bars represent SDs from three experiments. Statistical significance was determined by one-way ANOVA. ns, not significant; ***, $P < 0.001$.

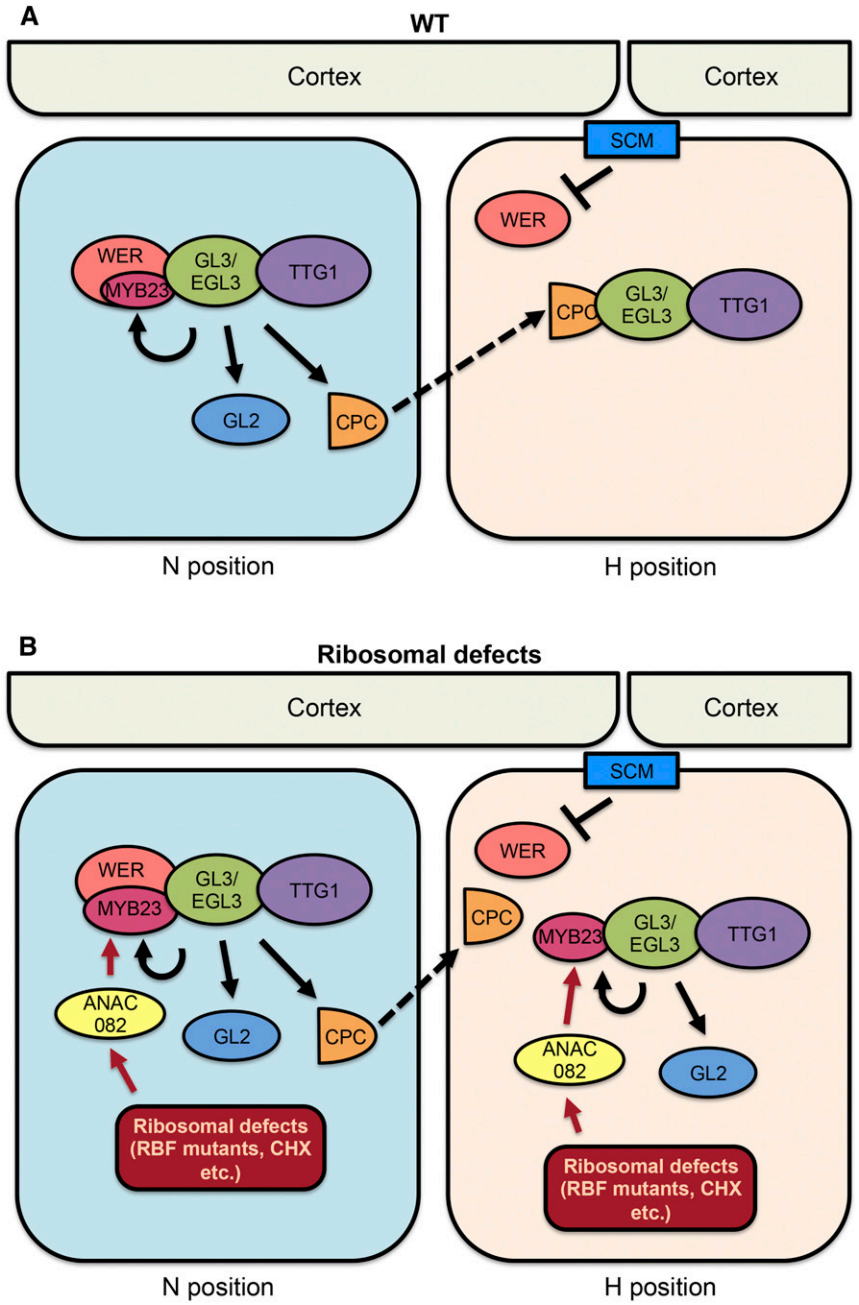

Figure 13. Working Models for Root Epidermal Cell Fate Regulation in Wild-Type Plants and Plants with Ribosomal Defects.

(A) In the wild-type (WT) root epidermis, the WER-GL3/EGL3-TTG1 complex preferentially accumulates in N-position cells, upregulating expression of *MYB23*, *GL2*, and *CPC*. MYB23 serves in a positive feedback loop to maintain WER function. GL2 promotes non-hair cell fate through repressing root hair genes. CPC is translocated to the adjacent H-position cell, where it inhibits WER's function by competitively binding to GL3/EGL3. SCM mediates inhibition of WER expression in H-position cells. Arrows indicate positive transcriptional regulation (black, direct; red, direct or indirect). Dashed black arrows indicate protein translocation.

(B) Ribosomal defects caused by RBF mutants or CHX treatment activate ANAC082, which results in additional *MYB23* expression in both H and N positions. The additional MYB23 in H-position cells helps to outcompete CPC, leading to excessive functional MYB23-GL3/EGL3-TTG1 complex and ectopic non-hair cell fate. Arrows indicate positive transcriptional regulation (black, direct; red, direct or indirect). Dashed black arrows indicate protein translocation.

components, differentially affect the translation of certain developmental regulator gene transcripts (Horiguchi et al., 2012). Indeed, the translation of several auxin response factors is modulated by particular RPs through the upstream open reading frame (uORF) in their 5′ UTRs (Rosado et al., 2012). ANAC082 has been identified as the mediator of several developmental phenotypes in RBF/RP mutants, connecting ribosomal health with a spectrum of developmental events (Ohbayashi et al., 2017; Ohbayashi and Sugiyama, 2018; Salomé, 2017). Notably, the *ANAC082* transcript possesses a uORF and therefore is potentially subject to translational regulation (Ohbayashi et al., 2017; Salomé, 2017). In addition, studies using the *ProANAC082*:*GUS* transcriptional reporter (Ohbayashi et al., 2017) and microarray analyses (Abbasi et al., 2010) as well as the quantitative real-time PCR reported in this study (Figure 7) suggest that *ANAC082* is also transcriptionally regulated in RBF mutants.

Ribosomal defects result from not only RBF/RP mutations but also challenging conditions such as nutrient deprivation, heat shock, and hypoxia (Mayer and Grummt, 2005; Golomb et al., 2014). In animal cells, ribosomal defects trigger ribosomal stress responses mediated by p53 activation and lead to cell cycle arrest and apoptosis (Zhang and Lu, 2009; Golomb et al., 2014; Penzo et al., 2019). As a potential plant version of this p53 pathway, ribosomal defects in plants lead to increased and/or activated ANAC082, which blocks tissue regeneration and delays seed germination (Supplemental Figure 1; Ohbayashi et al., 2017). Both tissue regeneration and seed germination involve massive cell proliferation and cell growth that rely heavily on ribosome activities. Therefore, the ANAC082-mediated effects on these processes could be a programmed response to contend with ribosomal defects.

In this study, we discovered that a switch of root epidermal cell fate is a common characteristic of several RBF mutants (*apum23*, *dim1A*, *prmt3*, and *apum24*) and plants treated with CHX (Figures 1, 8, and 11). However, these RBFs have been reported to have distinct and unrelated functions during rRNA splicing and rRNA modification (Abbasi et al., 2010; Wieckowski and Schiefelbein, 2012; Hang et al., 2014; Shanmugam et al., 2017), suggesting that this root epidermal phenotype is not due to specific molecular functions of these RBFs but is a developmental alteration commonly induced by ribosomal defects. The biological rationale for reducing root hair cell production in response to ribosomal defects is unclear. One possibility is that root hair cell differentiation requires a relatively high level of ribosome activity. It has been observed that during early developmental stages, cells in the H position show greater cell division rates, higher cytoplasmic densities, and delayed vacuolation compared with N-position cells (Galway et al., 1994; Berger et al., 1998). Furthermore, in this study, we discovered that H-position cells maintained larger nucleolar sizes and relatively greater amounts of APUM23 during later developmental stages (Figure 3). All these features suggest that developing H-position cells, committed to root hair production, are more metabolically active and so might have a greater demand for ribosomes. Accordingly, we hypothesize that a switch from root hair to non-hair cell fate may be part of a response program to accommodate for ribosomal defects.

Finally, we showed that flg22 treatment mimicked the effects of the RBF mutant by triggering ANAC082- and MYB23-dependent *GL2* expression in a WER-independent manner (Figure 12). This implies that a common regulatory module is used in the root epidermis to developmentally respond to two different stresses: ribosome biogenesis defects and plant defense. The rationale for this is unclear. It is possible that the defense response activates this regulatory module through its effects on ribosomes. Ribosome profiling has revealed that plants undergo translational reprogramming during the growth-to-defense transition (Meteignier et al., 2017; Xu et al., 2017a), which could impinge on ribosome biogenesis. Furthermore, bacterial pathogen infections alter translation of plant immune response regulators in a uORF-dependent manner (Xu et al., 2017b), suggesting the possibility that *ANAC082*, also bearing a uORF in its 5′ UTR (Ohbayashi et al., 2017), could be activated during plant defense. Further studies are required to clarify the relationship between these stress conditions and their effect on root epidermal cell fate.

METHODS

Plant Material and Growth Conditions

Arabidopsis (*Arabidopsis thaliana*) seeds were surface sterilized with 30% (v/v) bleach plus 0.02% (v/v) Triton X-100 and plated on mineral mix media previously reported by Schiefelbein and Somerville (1990) containing 0.3% (w/v) Gelrite. Seedling phenotypes were analyzed after 4 d of growth at 23°C under continuous light. For RBF mutants, older seedlings were used due to slower growth: *apum23-4* mutant, 8 d; *dim1a* mutant, 6 d; and *prmt3-1* mutant, 7 d. For RBF mutants carrying the *anac082-1* mutation, seedlings used for analysis were ~2 d younger than the corresponding RBF single mutants. For crosses and seed bulking, seedlings were transplanted to soil and grown under long-day light conditions (120 to 150 μmol m^{-2} s^{-1} with Osram L36W/840 Lumilux cool-white Hg bulbs) at 22°C (day) and 18°C (night).

For analysis of CHX-treated seedlings, seeds were grown on the standard mineral mix media for 4 d, transferred onto mineral mix media containing CHX (stock solution in ethanol), and grown for an additional 2 d before examination. For analysis of flg22-treated seedlings, seeds were directly grown on the standard mineral mix media containing 1 μM flg22 for 4 d before analysis.

The following mutant and reporter lines used in this study have been previously described: *wer-1* (Lee and Schiefelbein, 1999), *gl3* (Koornneef, 1981), *egl3* (Zhang et al., 2003), *ttg1* (Galway et al., 1994), *gl2-1* (Koornneef, 1981), *cpc-1* (Wada et al., 1997), *myb23-1* (Kirik et al., 2005), *dim1a* (Wieckowski and Schiefelbein, 2012), *ProGL2*:*GUS* (Masucci et al., 1996), *ProMYB23*:*GUS* (Kang et al., 2009), *ProMYB23*:*MYB23-GFP* (Kang et al., 2009), and *ProGL3*:*GL3-YFP* (Bernhardt et al., 2005). The *anac082-1* (*sriw1*) seeds were kindly provided by Munetaka Sugiyama. The *ProMYB23*:*MYB23-GFP* seeds were kindly provided by Myeong Min Lee.

The following mutant lines were reported previously and obtained from the Arabidopsis Biological Resource Center: *apum23-2* (*SALK_052992*; Abbasi et al., 2010), *apum24-2* (*SALK_033623*; Maekawa et al., 2018), *prmt3-1* (*SAIL_220_F08*; Hang et al., 2014), *prmt3-2* (*WISCDSLOX391A01*; Hang et al., 2014), and *anac082* (*GABI_282H08*; Kim et al., 2018).

Mutant Screening and Positional Cloning

Mutagenesis of *cpc-1* mutant seeds (Wassilewskija ecotype) with ethyl methanesulfonate was performed as previously described by Estelle and Somerville (1987). The *cpc-1 apum23-4* mutant (Wassilewskija ecotype) was crossed to plants of the Columbia ecotype to generate F2 and F3 offspring for positional cloning. Multiple simple sequence length

polymorphism and cleaved amplified polymorphic sequence markers were used (Jander et al., 2002). The responsible mutation was narrowed to a region between the CER481016 (27,196,516) and CER479543 (27,235,489) on chromosome 1. The protein-coding sequences of all genes within this interval were then cloned and sequenced to identify the mutated gene in *apum23-4*.

During later genetic studies, the derived cleaved amplified polymorphic sequences (Neff et al., 2002) strategy was used to identify the *apum23-4* mutation among individual plants in segregating populations. Genotyping primers are listed in Supplemental Table 2.

Transgenes and Plant Transformation

To construct the *ProAPUM23:APUM23-GFP* transgene, a 5.5-kb genomic fragment including 1-kb of the 5′ promoter region and the full-length genomic sequence of *APUM23* (with the stop codon removed) was cloned and integrated into the Gateway pENTR/SD/TOPO vector (Invitrogen), followed by subcloning into the Gateway binary vector pMDC107 (containing the C-terminal GFP tag). The cloning primers are listed in Supplemental Table 2.

To construct the *Pro35S:APUM23-YFP* transgene, a 4-kb genomic sequence of *APUM23* (starting from the ATG and replacing the stop codon with a Gly_5-Ala linker) was cloned and incorporated into the pCAM binary vector containing the 35S promoter at the 5′ end and an in-frame yellow fluorescent protein (YFP) tag at the 3′ end, using the NEBuilder HiFi DNA Assembly Cloning kit (New England Biolabs).

To construct the *ProFIB1:FIB1-mcherry* transgene, a 2.2-kb genomic fragment including 1 kb of the 5′ promoter region and the full-length *FIB1* genomic sequence (with the stop codon replaced with a Gly_5-Ala linker), a 0.7-kb mcherry sequence (with a stop codon added), and a 0.5-kb 3′ flanking region of *FIB1* were cloned and integrated together into the pCAM binary vector using the NEBuilder HiFi DNA Assembly Cloning kit. The mcherry tag was added to the C terminus of the *FIB1* genomic sequence. The cloning primers are listed in Supplemental Table 2.

To construct the *APUM23ρAPUM24* transgene, the 1.4-kb 5′ promoter region of *APUM23*, 4.1-kb full-length genomic region of *APUM24*, and 0.6-kb 3′ flanking region of *APUM23* were cloned and integrated into the pCAM binary vector using the NEBuilder HiFi DNA Assembly Cloning kit. The *ProAPUM24:APUM23* transgene was constructed using a similar strategy by assembling the 1-kb 5′ promoter region of *APUM24*, 3.6-kb full-length genomic region of *APUM23*, and 0.6-kb 3′ flanking region of *APUM24*. The cloning primers are listed in Supplemental Table 2.

Verified constructs were transformed into *Agrobacterium tumefaciens* strain GV3101, which was then used for plant transformation as described previously (Clough and Bent, 1998). After transformation, T1 seeds were harvested and screened for hygromycin resistance. Selected T2 seeds were grown and T3 seeds were tested to find homozygotes for insertions.

Microscopy, Quantification, and Image Analysis

Quantification of root hair cell and non-hair cell frequency were performed with a bright-field compound microscope using seedlings briefly stained with toluidine blue. Epidermal cell positions were determined according to their spatial relationship to underlying cortical cells. An epidermal cell in contact with two underlying cortical cells is in the H position, while an epidermal cell in contact with one underlying cortical cell is in the N position. For each genotype, 10 cells in the H position and 10 cells in the N position were scored per root, and 10 roots were used per replicate. Cell positions were determined according to their location with respect to underlying cortical cells. A cell was scored as a root hair cell if a visible protrusion was present on its cell surface, regardless of the length. A cell was scored as a non-hair cell if no root hair or initial root hair bulge was visible. At least three replicates were performed for each genotype in one experiment. Raw data from all experiments are listed in Supplemental Data Set 1. Depending on numbers of samples tested, statistical significance was determined using either one-way ANOVA or *t* test, and the results from all statistical tests are provided in Supplemental Data Set 2.

Histochemical analysis of seedling roots containing GUS reporter genes was performed as previously described (Masucci et al., 1996). For *ProGL2:GUS*, roots were stained with 0.1 mg/mL 5-bromo-4-chloro-3-indolyl-β-D-glucuronide substrates (CHX salt, GoldBio) at 37°C for 20 min, while for *ProMYB23:GUS*, roots were stained with 0.2 mg/mL 5-bromo-4-chloro-3-indolyl-β-D-glucuronide substrates at 37°C for 40 to 50 min. For quantification of *ProGL2:GUS* and *ProMYB23:GUS* expression, 10 continuous cells in the H position and 10 continuous cells in the N position were scored in each root, and 10 roots were used for each genotype in each replicate. The 10 cells included the first cell prior to rapid elongation (i.e., cell length > cell width) and extended shootward. A cell was scored as GUS positive if the GUS signal was visibly greater than the neighboring unstained H-position cells. Cell positions were defined according to their location with respect to underlying cortical cells. At least three replicates were performed for each genotype in one experiment. Raw data from all experiments are listed in Supplemental Data Set 1, and results of all statistical tests are provided in Supplemental Data Set 2.

Fluorescent images were obtained with a TCS SP5 DM6000B broadband confocal microscope (Leica) with an HCX PL APO CS 20× or 40× dry lens and facilitated with Leica Application Suite Advanced Fluorescence software. Before imaging, seedlings were stained with propidium iodide (PI) or DAPI and rinsed with water. Specifically, for DAPI staining, roots were incubated in 1/5000 dilution of fresh DAPI stock solution (5 mg/mL) for 15 to 20 min for nuclei visualization or for 1 to 2 min for cell wall visualization only. For GFP/PI imaging, an argon 488-nm laser was used for excitation. The GFP signal was collected under bandwidth 511 to 541 nm, the PI signal was collected under bandwidth 620 to 720 nm. For YFP/PI imaging, an argon 514-nm laser was used for excitation. The YFP signal was collected under bandwidth 528 to 547 nm. For DAPI/GFP/mcherry imaging, the 405-nm diode was used for DAPI excitation and the DPSS 561-nm laser was used for mcherry excitation. The DAPI signal was collected under bandwidth 424 to 475 nm, and the mcherry signal was collected under bandwidth 580 to 700 nm. The GFP and mcherry quantification was performed using ImageJ under separate RGB stacks, and the mcherry/GFP ratio was used for plotting.

To examine the expression of both the *ProGL2:GUS* and *ProMYB23:MYB23-GFP*/*ProGL3:GL3-YFP* markers within the same root, seedling roots were first imaged with the confocal microscope and then removed from slides and stained for GUS signals. Special care was taken to place the seedlings in the same posture for GUS examination as for the fluorescent imaging, taking advantage of unique root epidermal cell shapes as landmarks in the viewing window.

RNA Extraction and Quantitative Real-Time PCR

RNA extraction and quantitative real-time PCR were conducted as previously described (Wang et al., 2019). In general, ~2 mm of seedling root tips was harvested and RNA was extracted (RNeasy Plant Mini kit; QIAGEN). DNase I (RNase-free DNase set; QIAGEN) was applied to eliminate potential DNA contaminations in RNA samples, followed by cDNA synthesis (SuperScript First-Strand synthesis system; Invitrogen) and quantitative real-time PCR (Radiant Green Hi-ROX qPCR kit; Alkali Scientific). The PCR analysis and quantification were performed on the StepOnePlus Real Time System from Applied Biosystems following the Delta-Delta-Ct method. The *GAPCP2* gene (*AT1G16300*) was used as the internal reference. Primers used for qPCR are listed in Supplemental Table 2. Raw data from all experiments are listed in Supplemental Data Set 1, and the results from all statistical tests are provided in Supplemental Data Set 2.

Dual-Luciferase Assay

The dual-luciferase assay, tobacco (*Nicotiana tabacum*) infiltration, and luciferase activity measurement were performed as previously described (Liu et al., 2016). As the reporter, the *MYB23* promoter region (~2 kb, the same regulatory sequence used in the *ProMYB23*:*GUS* reporter described; Kirik et al., 2001) was cloned and integrated into the pGreen0800-LUC vector using a HiFi Assembly kit. As the effector, the *ANAC082* coding sequence was cloned and integrated into the pCAM vector driven by the *CaMV35S* promoter. Nucleotide primers are listed in Supplemental Table 2. The effector and reporter constructs were transformed into GV3101 *Agrobacterium*-competent cells. Overnight-cultured Agrobacteria carrying the correct constructs were resuspended in 10 mM $MgCl_2$ solution containing 0.5 μM acetosyringone. After a 2-h incubation at room temperature, resuspended Agrobacteria carrying effector and reporter constructs were mixed in a 5:1 ratio before infiltration.

Approximately 6-week-old tobacco plants were used for infiltration. For each combination of effector and reporter, at least three replicates were performed. For each replicate, at least six leaves were infiltrated. Raw data from all experiments are listed in Supplemental Data Set 1, and the results of all statistical tests are provided in Supplemental Data Set 2 . Plants were incubated in the dark for 24 h after infiltration, followed by another 1 to 2 d in regular growth conditions. The luciferase signals were detected using the Dual-Luciferase Reporter Assay System (Promega). For each leaf, pipette tips were used to collect a small piece of tissue close to the infiltrated spot. The leaf tissue was then crushed in 50-μL passive lysis buffer and incubated at room temperature for 10 min. The samples were placed in a luciferase microplate reader with the default settings for adding Luciferase Assay mix, reading luciferase activities, adding StopandGlo Reagen mix, and reading *Renilla* luciferase activities.

Accession Numbers

Arabidopsis sequence data from this article can be found in the GenBank/EMBL data libraries under the following accession numbers: APUM23 (AT1G72320), DIM1A (At2G47420), PRMT3 (AT3G12270), APUM24 (AT3G16810), ANAC082 (AT5G09330), CPC (At2G46410), FIB1 (At5G52470), GL2 (At1G79840), GL3 (At5g41315), EGL3 (AT1G63650), MYB23 (At5g40330), TTG1 (At5g24520), and WER (At5g14750).

SUPPLEMENTAL DATA

Supplemental Figure 1. RBF mutants exhibit delayed seed germination.

Supplemental Figure 2. The *apum23-4* mutant causes no significant alterations in root architecture.

Supplemental Figure 3. Additional representative roots with *ProAPUM23:APUM23-GFP* and *ProFIB1:FIB1-mcherry* reporters.

Supplemental Figure 4. Quantification of *ProGL2:GUS* signals in RBF double mutants with *wer-1*.

Supplemental Figure 5. Quantification of *ProMYB23:GUS* signals in RBF mutants *apum23-4*, *dim1a* and *prmt3-1.*

Supplemental Figure 6. ANAC082 is required for ectopic *MYB23* expression and ectopic non-hair cell specification in *apum23-4* and *dim1a* mutants.

Supplemental Figure 7. Dual luciferase assay showing effect of ANAC082 on *MYB23* promoter activity in tobacco leaves.

Supplemental Figure 8. Quantification of *ProGL2:GUS* signals in seedling root tips of wild type, *prmt3-1* and *apum24-2* mutants.

Supplemental Table 1. A list of the RBF mutants examined in this study.

Supplemental Table 2. Primers used for genotyping, cloning, and qPCR.

Supplemental Data Set 1. Raw data for quantification of root epidermal cell specification, *ProGL2:GUS* or *ProMYB23:GUS* expression, and qPCR in this study.

Supplemental Data Set 2. P-values of one-way ANOVA tests and *t* tests used in this study.

ACKNOWLEDGMENTS

We thank Myeong Min Lee (Yonsei University, Korea) for the kind gift of the *ProMYB23:MYB23-GFP* seeds and Munetaka Sugiyama for the *anac082-1* seeds. We thank Chaoyang Liu (South China Agricultural University, China) for the kind gift of the pGreen0800-LUC construct. We thank The Arabidopsis Biological Resource Center for providing seed stocks of multiple mutant lines. We thank Erik Nielsen, Andrej Wierzbicki, and Jairam Menon (University of Michigan, Ann Arbor) for suggestions and informative discussion. We thank Gregg Soboccinski (University of Michigan, Ann Arbor) for technical assistance with microscopy. This work was supported by the National Science Foundation (grant IOS-1444400).

AUTHOR CONTRIBUTIONS

W.W., K.H.R., A.B., and C.B. conducted the experiments. W.W., K.H.R., and A.B. analyzed the data. J.S. supervised the experiments. W.W., K.H.R., A.B., and J.S. contributed to the design of the project. W.W. and J.S. wrote the article with contributions from A.B., K.H.R., and C.B.

Received October 2, 2019; revised March 30, 2020; accepted April 29, 2020; published May 5, 2020.

REFERENCES

Abbasi, N., Kim, H.B., Park, N.I., Kim, H.S., Kim, Y.K., Park, Y.I., and Choi, S.B. (2010). APUM23, a nucleolar Puf domain protein, is involved in pre-ribosomal RNA processing and normal growth patterning in Arabidopsis. Plant J. **64:** 960–976.

Balkunde, R., Pesch, M., and Hülskamp, M. (2010). Trichome patterning in *Arabidopsis thaliana* from genetic to molecular models. Curr. Top. Dev. Biol. **91:** 299–321.

Berger, F., Hung, C.Y., Dolan, L., and Schiefelbein, J. (1998). Control of cell division in the root epidermis of *Arabidopsis thaliana*. Dev. Biol. **194:** 235–245.

Bernhardt, C., Lee, M.M., Gonzalez, A., Zhang, F., Lloyd, A., and Schiefelbein, J. (2003). The bHLH genes GLABRA3 (GL3) and ENHANCER OF GLABRA3 (EGL3) specify epidermal cell fate in the Arabidopsis root. Development **130:** 6431–6439.

Bernhardt, C., Zhao, M., Gonzalez, A., Lloyd, A., and Schiefelbein, J. (2005). The bHLH genes GL3 and EGL3 participate in an intercellular regulatory circuit that controls cell patterning in the Arabidopsis root epidermis. Development **132:** 291–298.

Bruex, A., Kainkaryam, R.M., Wieckowski, Y., Kang, Y.H., Bernhardt, C., Xia, Y., Zheng, X., Wang, J.Y., Lee, M.M., Benfey, P., Woolf, P.J., and Schiefelbein, J. (2012). A gene regulatory network for root epidermis cell differentiation in Arabidopsis. PLoS Genet. **8:** e1002446.

Byrne, M.E. (2009). A role for the ribosome in development. Trends Plant Sci. **14:** 512–519.

Clough, S.J., and Bent, A.F. (1998). Floral dip: A simplified method for *Agrobacterium*-mediated transformation of *Arabidopsis thaliana*. Plant J. **16:** 735–743.

Clowes, F.A.L. (2000). Pattern in root meristem development in angiosperms. New Phytol. **146:** 83–94.

Cvrčková, F., Bezvoda, R., and Zárský, V. (2010). Computational identification of root hair-specific genes in Arabidopsis. Plant Signal. Behav. **5:** 1407–1418.

de Kloet, S.R. (1966). Ribonucleic acid synthesis in yeast. The effect of cycloheximide on the synthesis of ribonucleic acid in *Saccharomyces carlsbergensis*. Biochem. J. **99:** 566–581.

Duckett, C.M., Grierson, C., Linstead, P., Schneider, K., Lawson, E., Dean, C., Poethig, S., and Roberts, K. (1994). Clonal relationships and cell patterning in the root epidermis of Arabidopsis. Development **120:** 2465.

Edwards, T.A., Pyle, S.E., Wharton, R.P., and Aggarwal, A.K. (2001). Structure of Pumilio reveals similarity between RNA and peptide binding motifs. Cell **105:** 281–289.

Ernst, H.A., Olsen, A.N., Larsen, S., and Lo Leggio, L. (2004). Structure of the conserved domain of ANAC, a member of the NAC family of transcription factors. EMBO Rep. **5:** 297–303.

Estelle, M.A., and Somerville, C. (1987). Auxin-resistant mutants of *Arabidopsis thaliana* with an altered morphology. Mol. Gen. Genet. **206:** 200–206.

Ferrari, S., Galletti, R., Denoux, C., De Lorenzo, G., Ausubel, F.M., and Dewdney, J. (2007). Resistance to *Botrytis cinerea* induced in Arabidopsis by elicitors is independent of salicylic acid, ethylene, or jasmonate signaling but requires PHYTOALEXIN DEFICIENT3. Plant Physiol. **144:** 367–379.

Francischini, C.W., and Quaggio, R.B. (2009). Molecular characterization of *Arabidopsis thaliana* PUF proteins--binding specificity and target candidates. FEBS J. **276:** 5456–5470.

Galway, M.E., Masucci, J.D., Lloyd, A.M., Walbot, V., Davis, R.W., and Schiefelbein, J.W. (1994). The TTG gene is required to specify epidermal cell fate and cell patterning in the Arabidopsis root. Dev. Biol. **166:** 740–754.

Golomb, L., Volarevic, S., and Oren, M. (2014). p53 and ribosome biogenesis stress: The essentials. FEBS Lett. **588:** 2571–2579.

Gómez-Gómez, L., Felix, G., and Boller, T. (1999). A single locus determines sensitivity to bacterial flagellin in *Arabidopsis thaliana*. Plant J. **18:** 277–284.

Hang, R., Liu, C., Ahmad, A., Zhang, Y., Lu, F., and Cao, X. (2014). Arabidopsis protein arginine methyltransferase 3 is required for ribosome biogenesis by affecting precursor ribosomal RNA processing. Proc. Natl. Acad. Sci. USA **111:** 16190–16195.

Harscoët, E., Dubreucq, B., Palauqui, J.C., and Lepiniec, L. (2010). NOF1 encodes an Arabidopsis protein involved in the control of rRNA expression. PLoS One **5:** e12829.

Horiguchi, G., Van Lijsebettens, M., Candela, H., Micol, J.L., and Tsukaya, H. (2012). Ribosomes and translation in plant developmental control. Plant Sci. **191–192:** 24–34.

Huang, L., Shi, X., Wang, W., Ryu, K.H., and Schiefelbein, J. (2017). Diversification of root hair development genes in vascular plants. Plant Physiol. **174:** 1697–1712.

Huang, T., Kerstetter, R.A., and Irish, V.F. (2014). APUM23, a PUF family protein, functions in leaf development and organ polarity in Arabidopsis. J. Exp. Bot. **65:** 1181–1191.

Jander, G., Norris, S.R., Rounsley, S.D., Bush, D.F., Levin, I.M., and Last, R.L. (2002). Arabidopsis map-based cloning in the post-genome era. Plant Physiol. **129:** 440–450.

Kalinina, N.O., Makarova, S., Makhotenko, A., Love, A.J., and Taliansky, M. (2018). The multiple functions of the nucleolus in plant development, disease and stress responses. Front Plant Sci **9:** 132.

Kang, Y.H., Kirik, V., Hulskamp, M., Nam, K.H., Hagely, K., Lee, M.M., and Schiefelbein, J. (2009). The MYB23 gene provides a positive feedback loop for cell fate specification in the Arabidopsis root epidermis. Plant Cell **21:** 1080–1094.

Kim, H.J., Park, J.H., Kim, J., Kim, J.J., Hong, S., Kim, J., Kim, J.H., Woo, H.R., Hyeon, C., Lim, P.O., Nam, H.G., and Hwang, D. (2018). Time-evolving genetic networks reveal a NAC troika that negatively regulates leaf senescence in *Arabidopsis*. Proc. Natl. Acad. Sci. USA **115:** E4930–E4939.

Kirik, V., Lee, M.M., Wester, K., Herrmann, U., Zheng, Z., Oppenheimer, D., Schiefelbein, J., and Hulskamp, M. (2005). Functional diversification of MYB23 and GL1 genes in trichome morphogenesis and initiation. Development **132:** 1477–1485.

Kirik, V., Schnittger, A., Radchuk, V., Adler, K., Hülskamp, M., and Bäumlein, H. (2001). Ectopic expression of the Arabidopsis AtMYB23 gene induces differentiation of trichome cells. Dev. Biol. **235:** 366–377.

Kirik, V., Simon, M., Huelskamp, M., and Schiefelbein, J. (2004). The ENHANCER OF TRY AND CPC1 gene acts redundantly with TRIPTYCHON and CAPRICE in trichome and root hair cell patterning in Arabidopsis. Dev. Biol. **268:** 506–513.

Koornneef, M. (1981). The complex syndrome of ttg mutants. Arab. Inf. Serv. **18:** 45–51.

Kurata, T., et al. (2005). Cell-to-cell movement of the CAPRICE protein in Arabidopsis root epidermal cell differentiation. Development **132:** 5387–5398.

Kwak, S.H., and Schiefelbein, J. (2008). A feedback mechanism controlling SCRAMBLED receptor accumulation and cell-type pattern in Arabidopsis. Curr. Biol. **18:** 1949–1954.

Kwak, S.H., Shen, R., and Schiefelbein, J. (2005). Positional signaling mediated by a receptor-like kinase in Arabidopsis. Science **307:** 1111–1113.

Lange, H., Sement, F.M., and Gagliardi, D. (2011). MTR4, a putative RNA helicase and exosome co-factor, is required for proper rRNA biogenesis and development in *Arabidopsis thaliana*. Plant J. **68:** 51–63.

Lee, M.M., and Schiefelbein, J. (1999). WEREWOLF, a MYB-related protein in Arabidopsis, is a position-dependent regulator of epidermal cell patterning. Cell **99:** 473–483.

Lee, M.M., and Schiefelbein, J. (2002). Cell pattern in the Arabidopsis root epidermis determined by lateral inhibition with feedback. Plant Cell **14:** 611–618.

Li, S.F., Milliken, O.N., Pham, H., Seyit, R., Napoli, R., Preston, J., Koltunow, A.M., and Parish, R.W. (2009). The Arabidopsis MYB5 transcription factor regulates mucilage synthesis, seed coat development, and trichome morphogenesis. Plant Cell **21:** 72–89.

Lin, Q., Ohashi, Y., Kato, M., Tsuge, T., Gu, H., Qu, L.J., and Aoyama, T. (2015). GLABRA2 directly suppresses basic helix-loop-helix transcription factor genes with diverse functions in root hair development. Plant Cell **27:** 2894–2906.

Liu, C., Long, J., Zhu, K., Liu, L., Yang, W., Zhang, H., Li, L., Xu, Q., and Deng, X. (2016). Characterization of a citrus R2R3-MYB transcription factor that regulates the flavonol and hydroxycinnamic acid biosynthesis. Sci. Rep. **6:** 25352.

Maekawa, S., Ishida, T., and Yanagisawa, S. (2018). Reduced expression of *APUM24*, encoding a novel rRNA processing factor, induces sugar-dependent nucleolar stress and altered sugar responses in *Arabidopsis thaliana*. Plant Cell **30:** 209–227.

Masucci, J.D., Rerie, W.G., Foreman, D.R., Zhang, M., Galway, M.E., Marks, M.D., and Schiefelbein, J.W. (1996). The homeobox gene GLABRA2 is required for position-dependent cell differentiation in the root epidermis of *Arabidopsis thaliana*. Development **122:** 1253–1260.

Mayer, C., and Grummt, I. (2005). Cellular stress and nucleolar function. Cell Cycle **4:** 1036–1038.

Meteignier, L.V., El Oirdi, M., Cohen, M., Barff, T., Matteau, D., Lucier, J.F., Rodrigue, S., Jacques, P.E., Yoshioka, K., and Moffett, P. (2017). Translatome analysis of an NB-LRR immune response identifies important contributors to plant immunity in Arabidopsis. J. Exp. Bot. **68:** 2333–2344.

Missbach, S., Weis, B.L., Martin, R., Simm, S., Bohnsack, M.T., and Schleiff, E. (2013). 40S Ribosome biogenesis co-factors are essential for gametophyte and embryo development. PLoS One **8:** e54084.

Müller, M., and Schmidt, W. (2004). Environmentally induced plasticity of root hair development in Arabidopsis. Plant Physiol. **134:** 409–419.

Murata, Y., and Wharton, R.P. (1995). Binding of pumilio to maternal hunchback mRNA is required for posterior patterning in Drosophila embryos. Cell **80:** 747–756.

Neff, M.M., Turk, E., and Kalishman, M. (2002). Web-based primer design for single nucleotide polymorphism analysis. Trends Genet. **18:** 613–615.

Ohashi, Y., Oka, A., Rodrigues-Pousada, R., Possenti, M., Ruberti, I., Morelli, G., and Aoyama, T. (2003). Modulation of phospholipid signaling by GLABRA2 in root-hair pattern formation. Science **300:** 1427–1430.

Ohbayashi, I., Konishi, M., Ebine, K., and Sugiyama, M. (2011). Genetic identification of Arabidopsis RID2 as an essential factor involved in pre-rRNA processing. Plant J. **67:** 49–60.

Ohbayashi, I., Lin, C.Y., Shinohara, N., Matsumura, Y., Machida, Y., Horiguchi, G., Tsukaya, H., and Sugiyama, M. (2017). Evidence for a role of ANAC082 as a ribosomal stress response mediator leading to growth defects and developmental alterations in Arabidopsis. Plant Cell **29:** 2644–2660.

Ohbayashi, I., and Sugiyama, M. (2018). Plant nucleolar stress response, a new face in the NAC-dependent cellular stress responses. Front Plant Sci **8:** 2247.

Olsen, A.N., Ernst, H.A., Lo Leggio, L., Johansson, E., Larsen, S., and Skriver, K. (2004). Preliminary crystallographic analysis of the NAC domain of ANAC, a member of the plant-specific NAC transcription factor family. Acta Crystallogr. D Biol. Crystallogr. **60:** 112–115.

Ooka, H., et al. (2003). Comprehensive analysis of NAC family genes in Oryza sativa and Arabidopsis thaliana. DNA Res. **10:** 239–247.

Penzo, M., Montanaro, L., Treré, D., and Derenzini, M. (2019). The ribosome biogenesis-cancer connection. Cells **8:** 8.

Pih, K.T., Yi, M.J., Liang, Y.S., Shin, B.J., Cho, M.J., Hwang, I., and Son, D. (2000). Molecular cloning and targeting of a fibrillarin homolog from Arabidopsis. Plant Physiol. **123:** 51–58.

Pontvianne, F., et al. (2010). Nucleolin is required for DNA methylation state and the expression of rRNA gene variants in *Arabidopsis thaliana*. PLoS Genet. **6:** e1001225.

Qiu, C., McCann, K.L., Wine, R.N., Baserga, S.J., and Hall, T.M. (2014). A divergent Pumilio repeat protein family for pre-rRNA processing and mRNA localization. Proc. Natl. Acad. Sci. USA **111:** 18554–18559.

Rishmawi, L., Wolff, H., Schrader, A., and Hülskamp, M. (2018). Sub-epidermal expression of *ENHANCER OF TRIPTYCHON AND CAPRICE1* and its role in root hair formation upon Pi starvation. Front. Plant Sci. **9:** 1411.

Rosado, A., Li, R., van de Ven, W., Hsu, E., and Raikhel, N.V. (2012). Arabidopsis ribosomal proteins control developmental programs through translational regulation of auxin response factors. Proc. Natl. Acad. Sci. USA **109:** 19537–19544.

Ryu, K.H., Kang, Y.H., Park, Y.H., Hwang, I., Schiefelbein, J., and Lee, M.M. (2005). The WEREWOLF MYB protein directly regulates CAPRICE transcription during cell fate specification in the Arabidopsis root epidermis. Development **132:** 4765–4775.

Sáez-Vásquez, J., and Delseny, M. (2019). Ribosome biogenesis in plants: From functional 45S ribosomal DNA organization to ribosome assembly factors. Plant Cell **31:** 1945–1967.

Salomé, P.A. (2017). Proliferate at your own risk: Ribosomal stress and regeneration. Plant Cell **29:** 2318.

Schiefelbein, J., Huang, L., and Zheng, X. (2014). Regulation of epidermal cell fate in Arabidopsis roots: The importance of multiple feedback loops. Front Plant Sci **5:** 47.

Schiefelbein, J.W., and Somerville, C. (1990). Genetic control of root hair development in *Arabidopsis thaliana*. Plant Cell **2:** 235–243.

Schmidt, W., and Schikora, A. (2001). Different pathways are involved in phosphate and iron stress-induced alterations of root epidermal cell development. Plant Physiol. **125:** 2078–2084.

Shanmugam, T., Abbasi, N., Kim, H.S., Kim, H.B., Park, N.I., Park, G.T., Oh, S.A., Park, S.K., Muench, D.G., Choi, Y., Park, Y.I., and Choi, S.B. (2017). An Arabidopsis divergent pumilio protein, APUM24, is essential for embryogenesis and required for faithful pre-rRNA processing. Plant J. **92:** 1092–1105.

Simon, M., Lee, M.M., Lin, Y., Gish, L., and Schiefelbein, J. (2007). Distinct and overlapping roles of single-repeat MYB genes in root epidermal patterning. Dev. Biol. **311:** 566–578.

Song, S.K., Ryu, K.H., Kang, Y.H., Song, J.H., Cho, Y.H., Yoo, S.D., Schiefelbein, J., and Lee, M.M. (2011). Cell fate in the Arabidopsis root epidermis is determined by competition between WEREWOLF and CAPRICE. Plant Physiol. **157:** 1196–1208.

Stoyanova, B.B., and Hadjiolov, A.A. (1979). Alterations in the processing of rat-liver ribosomal RNA caused by cycloheximide inhibition of protein synthesis. Eur. J. Biochem. **96:** 349–356.

Stracke, R., Werber, M., and Weisshaar, B. (2001). The R2R3-MYB gene family in *Arabidopsis thaliana*. Curr. Opin. Plant Biol. **4:** 447–456.

Szostak, E., and Gebauer, F. (2013). Translational control by 3′-UTR-binding proteins. Brief. Funct. Genomics **12:** 58–65.

Tam, P.P., Barrette-Ng, I.H., Simon, D.M., Tam, M.W., Ang, A.L., and Muench, D.G. (2010). The Puf family of RNA-binding proteins in plants: phylogeny, structural modeling, activity and subcellular localization. BMC Plant Biol. **10:** 44.

Thomson, E., Ferreira-Cerca, S., and Hurt, E. (2013). Eukaryotic ribosome biogenesis at a glance. J. Cell Sci. **126:** 4815–4821.

Thomson, E., Rappsilber, J., and Tollervey, D. (2007). Nop9 is an RNA binding protein present in pre-40S ribosomes and required for 18S rRNA synthesis in yeast. RNA **13:** 2165–2174.

Tominaga, R., Iwata, M., Okada, K., and Wada, T. (2007). Functional analysis of the epidermal-specific MYB genes CAPRICE and WEREWOLF in Arabidopsis. Plant Cell **19:** 2264–2277.

Wada, T., Kurata, T., Tominaga, R., Koshino-Kimura, Y., Tachibana, T., Goto, K., Marks, M.D., Shimura, Y., and Okada, K. (2002). Role of a positive regulator of root hair development, CAPRICE, in Arabidopsis root epidermal cell differentiation. Development **129:** 5409–5419.

Wada, T., Tachibana, T., Shimura, Y., and Okada, K. (1997). Epidermal cell differentiation in Arabidopsis determined by a Myb homolog, CPC. Science **277:** 1113–1116.

Wang, M., Ogé, L., Perez-Garcia, M.D., Hamama, L., and Sakr, S. (2018). The PUF protein family: Overview on PUF RNA targets,

biological functions, and post transcriptional regulation. Int. J. Mol. Sci. **19:** 19.

Wang, W., Ryu, K.H., Barron, C., and Schiefelbein, J. (2019). Root epidermal cell patterning is modulated by a critical residue in the WEREWOLF transcription factor. Plant Physiol. **181:** 1239–1256.

Wang, Y., Zhang, W., Li, K., Sun, F., Han, C., Wang, Y., and Li, X. (2008). Salt-induced plasticity of root hair development is caused by ion disequilibrium in *Arabidopsis thaliana*. J. Plant Res. **121:** 87–96.

Weis, B.L., Kovacevic, J., Missbach, S., and Schleiff, E. (2015a). Plant-specific features of ribosome biogenesis. Trends Plant Sci. **20:** 729–740.

Weis, B.L., Missbach, S., Marzi, J., Bohnsack, M.T., and Schleiff, E. (2014). The 60S associated ribosome biogenesis factor LSG1-2 is required for 40S maturation in *Arabidopsis thaliana*. Plant J. **80:** 1043–1056.

Weis, B.L., Palm, D., Missbach, S., Bohnsack, M.T., and Schleiff, E. (2015b). atBRX1-1 and atBRX1-2 are involved in an alternative rRNA processing pathway in *Arabidopsis thaliana*. RNA **21:** 415–425.

Wickens, M., Bernstein, D.S., Kimble, J., and Parker, R. (2002). A PUF family portrait: 3'UTR regulation as a way of life. Trends Genet. **18:** 150–157.

Wieckowski, Y., and Schiefelbein, J. (2012). Nuclear ribosome biogenesis mediated by the DIM1A rRNA dimethylase is required for organized root growth and epidermal patterning in Arabidopsis. Plant Cell **24:** 2839–2856.

Winter, D., Vinegar, B., Nahal, H., Ammar, R., Wilson, G.V., and Provart, N.J. (2007). An "Electronic Fluorescent Pictograph" browser for exploring and analyzing large-scale biological data sets. PLoS One **2:** e718.

Xu, G., Greene, G.H., Yoo, H., Liu, L., Marqués, J., Motley, J., and Dong, X. (2017a). Global translational reprogramming is a fundamental layer of immune regulation in plants. Nature **545:** 487–490.

Xu, G., Yuan, M., Ai, C., Liu, L., Zhuang, E., Karapetyan, S., Wang, S., and Dong, X. (2017b). uORF-Mediated translation allows engineered plant disease resistance without fitness costs. Nature **545:** 491–494.

Yamaguchi, M., Nagahage, I.S.P., Ohtani, M., Ishikawa, T., Uchimiya, H., Kawai-Yamada, M., and Demura, T. (2015). Arabidopsis NAC domain proteins VND-INTERACTING1 and ANAC103 interact with multiple NAC domain proteins. Plant Biotechnol. **32:** 119–132.

Zamore, P.D., Williamson, J.R., and Lehmann, R. (1997). The Pumilio protein binds RNA through a conserved domain that defines a new class of RNA-binding proteins. RNA **3:** 1421–1433.

Zhang, C., and Muench, D.G. (2015). A nucleolar PUF RNA-binding protein with specificity for a unique RNA sequence. J. Biol. Chem. **290:** 30108–30118.

Zhang, F., Gonzalez, A., Zhao, M., Payne, C.T., and Lloyd, A. (2003). A network of redundant bHLH proteins functions in all TTG1-dependent pathways of Arabidopsis. Development **130:** 4859–4869.

Zhang, J., McCann, K.L., Qiu, C., Gonzalez, L.E., Baserga, S.J., and Hall, T.M. (2016). Nop9 is a PUF-like protein that prevents premature cleavage to correctly process pre-18S rRNA. Nat. Commun. **7:** 13085.

Zhang, Y., and Lu, H. (2009). Signaling to p53: Ribosomal proteins find their way. Cancer Cell **16:** 369–377.